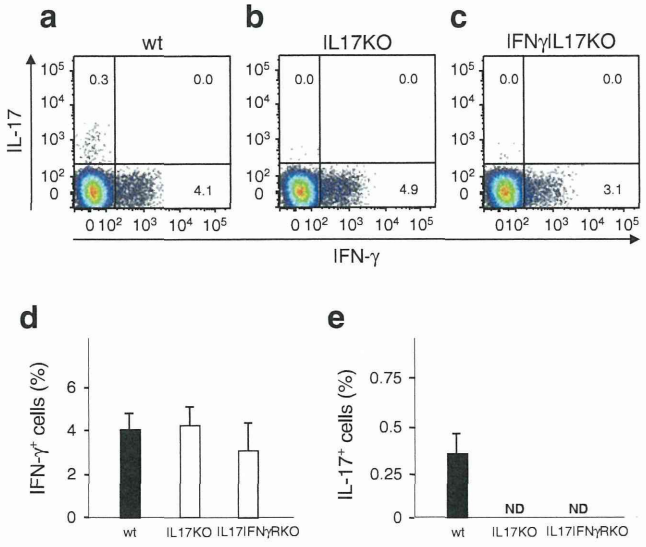

Fig. 3 IFN-γ positive or IL-17 positive cells in $CD4^+$ SPCs in the IL-17-deficient and IL-17/IFN-γR-deficient NOD mice. SPCs were prepared, stimulated with PMA and ionomycin for 5 h, stained for cell surface CD4 and intracellular IFN-γ and IL-17, and analysed with flow cytometry (**a**–**c**). Representative staining of $CD4^+$ SPCs for intracellular IFN-γ and/or IL-17. (**d**,**e**) Numeration of Th1 and Th17 cells, respectively. The data are means±SD (n=5). KO, knockout; ND, not detected

mice of the same age (Fig. 2a). However, such attenuation of diabetes development by IL-17-deficient diabetogenic T cells was no longer seen after a similar transfer of the same cells derived from older non-diabetic or diabetic mice (Fig. 2b,c). Taken together, the present results suggest that IL-17 participates in the pathogenesis of the early phase of the development of diabetes, but elimination of IL-17 could be readily dispensable in the late phase of diabetes.

In vitro-polarised Th17 cells derived from BDC2.5 TCR-Tg NOD mice do not transfer diabetes in newborn NOD mice but do transfer diabetes in immune-deficient hosts through conversion into Th1 cells or Th1/Th17 cells coexpressing Th1 and Th17 cytokines [23, 24]. We hypothesised that such a conversion of Th17 into Th1 cells or Th1/Th17 cells may have compensated for the disease inhibition by IL-17 single deficiency in NOD mice in the present study. To test our hypothesis, we also evaluated the impact of the genetic deletion of both IL-17 and IFN-γ signalling in NOD mice to determine whether such a double deficiency could clearly suppress disease. As hypothesised, IL-17/IFN-γR double deficiency significantly suppressed the longstanding incidence of diabetes compared with IL-17 single deficiency in NOD mice (Fig. 1a). These results indicate that Th1 and Th17 cytokines may synergistically contribute to the development of diabetes in NOD mice, since IFN-γR-deficient NOD mice exhibit minimal or no inhibition of disease [10, 28].

We fortuitously found that IL-17/IFN-γR double-deficient NOD mice had a severe lymphopenic phenotype. A previous study demonstrated that wt NOD mice have mild lymphopenia compared with a non-autoimmune strain, and, as a result, compensatory homeostatic expansion of T cells generates anti-islet autoimmunity resulting in the development of diabetes [29]. In contrast, NOD mice harbouring a C57BL/6-derived *Idd3* genetic interval (which encodes the *Il2* and *Il21* genes) (NOD.*Idd3* mice) are disease-resistant and not lymphopenic. It has recently been shown that naive T cells from NOD mice exhibit a greater propensity to differentiate into Th17 cells than those from NOD.*Idd3* mice, and IL-21 signalling in antigen-presenting cells plays a central role in such Th17 cell development [30].

On the other hand, several studies have demonstrated that diabetes susceptibility and protection in NOD mice correlate with lymphopenia and homeostatic expansion under a variety of experimental conditions. Thymectomy at weaning or treatment with cyclophosphamide, which causes lymphocyte apoptosis, accelerates diabetes onset in NOD mice

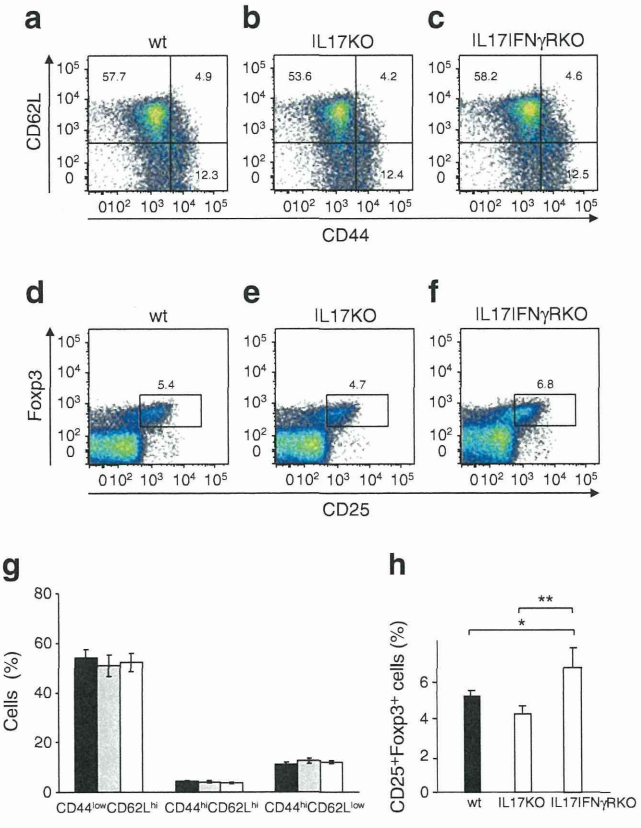

Fig. 4 Activation markers and $CD25^+Foxp3^+$cells in $CD4^+$ SPCs. Unstimulated SPCs were stained for cell surface CD4, CD62L, CD44 and CD25, and intracellular Foxp3 and analysed with flow cytometry. Representative staining of $CD4^+$ SPCs for (**a**–**c**) CD62L and CD44 and (**d**–**f**) CD25 and Foxp3. Numeration of (**g**) each $CD44^{low}CD62L^{hi}$, $CD44^{hi}CD62L^{hi}$ and $CD44^{hi}CD62L^{low}$ cells in wt NOD mice (black bar), *Il17*$^{-/-}$/*Ifngr1*$^{+/+}$ NOD mice (solid grey) and *Il17*$^{-/-}$/*Ifngr1*$^{-/-}$ NOD mice (white bar) and (**h**) $CD25^+Foxp3^+$ cells. The data are mean±SD (n=5), and group differences were analysed by Mann–Whitney U test. *p<0.05, **p<0.01. KO, knockout

[31, 32]. In contrast, immunisation with complete Freund's adjuvant (CFA) increases T cell numbers and protects NOD mice from diabetes [29, 33]. Mori et al have reported that IFN-γR deficiency abrogates cyclophosphamide-induced acceleration of diabetes and CFA-mediated protection in NOD mice [34, 35]. Thus, Th17 cell development and IFN-γ signalling may play a critical role in diabetes susceptibility mediated by lymphopenia-induced homeostatic expansion in NOD mice, although the precise kinetics and mechanisms of severe lymphopenia in these mice are still being elucidated.

We also found that double-deficient NOD mice had a preferential increase in Tregs among $CD4^+$ splenic T cells. Several recent findings highlight the plasticity within the $CD4^+$ Th cell population including Th1, Th2, Th17 and Tregs, and Th17 cells and Tregs are more plastic than Th1/Th2 cells [21]. Networks of cytokines are critical for determining $CD4^+$ T cell fates and effector cytokines [36]. For example, Bertin-Maghit et al clearly demonstrated that systemic overproduction of IL-1β in 6- to 16-week-old NOD mice impairs Treg function and promotes the Treg to Th17 conversion [37]. A pair of studies showed that Th17 cells generated ex vivo or in vitro can be converted into the Th1 phenotype by combined IFN-γ and IL-12 signalling through epigenetic processes [38, 39]. As described above, in vitro-polarised Th17 cells are readily reprogrammed into other T cell lineages on transfer into lymphopenic hosts [23, 40]. Of note, treatment with cyclophosphamide not only fails to accelerate diabetes but also confers permanent protection against diabetes by the preferential generation of Tregs in IFN-γR-deficient NOD mice [34]. It is possible that IFN-γR deficiency under lymphopenic conditions inhibits such a Th shift from Th1 to Th17 or from Tregs to another Teff lineage, resulting in a preferential increase in the Treg population and disease resistance in our double-deficient NOD mice.

Thus, we have here demonstrated that IL-17/Th17 participates in the development of insulitis and that both IL-17 and IFN-γ signalling may synergistically contribute to the Teff/Treg balance to Teffs during homeostasis expansion and the subsequent development of diabetes in NOD mice.

From the clinical point of view, the therapeutic efficacy of the inhibition of Th17 cells in some autoimmune diseases has been demonstrated [18, 19]. It has been reported that children with new-onset type 1 diabetes have an increased proportion of memory $CD4^+$ cells that have increased IL-17 secretion, suggesting that upregulation of Th17 immunity is associated with human type 1 diabetes [41, 42]. This implies a novel potential therapeutic strategy for human type 1 diabetes based on the control of IL-17 immunity. However, the results presented in the present study indicate that a single blockade of an effector cytokine such as IL-17 or IFN-γ readily compensates for the Th shift from Tregs to effector Th lineage through multiple networks of cytokines. The appropriate timing or therapeutic strategy for inhibiting the Treg/Teff conversion—such as a combination blockade of multiple cytokines or transcriptional factors such as the Janus kinase (JAK)–signal transducers and activator of transcription (STAT) pathway, Runx3 and IRF-4—should be carefully considered with the goal of preventing or delaying the development of type 1 diabetes [36].

Acknowledgements We thank O. Kanagawa for providing IFN-γR-deficient NOD mice and M. Motomura and Y. Kataoka for their technical assistance. G. S. Eisenbarth, who was executive director of the Barbara Davis Center for Diabetes, contributed greatly to the early experiments of the study before his untimely death.

Funding This work was supported by research grants from the Japan Society for the Promotion of Science (Nos 24591334, 21591143, 23791036 and 22790865).

Duality of interest The authors declare that there is no duality of interest associated with this manuscript.

Contribution statement All authors contributed to the conception and design of the study, acquisition, analysis and interpretation of data, and drafting and editing of the manuscript. All of the authors approved the final version of the manuscript. GK, MK and NA had full access to all of the data in the study and take responsibility for the integrity of the data and the accuracy of the data analysis.

References

1. Eisenbarth GS, Vardi P, Ziegler AG et al (1988) Lessons from the NOD mouse and BB rat: similarities and contrasts. In: Renold AE, Shafir E (eds) Frontiers in diabetes research: lessons from animal diabetes: II. John Libbey, London
2. Rabinovitch A, Suarez-Pinzon WL, Sorensen O, Bleackley RC, Power RF (1995) IFN-gamma gene expression in pancreatic islet-infiltrating mononuclear cells correlates with autoimmune diabetes in nonobese diabetic mice. J Immunol 154:4874–4882
3. Suarez-Pinzon W, Rajotte RV, Mosmann TR, Rabinovitch A (1996) Both CD4+ and CD8+ T cells in syngeneic islet grafts in NOD mice produce interferon-γ during β-cell destruction. Diabetes 45:1350–1357
4. Haskins K, Wegmann D (1996) Diabetogenic T cell clones. Diabetes 45:1299–1305
5. Haskins K (2005) Pathogenic T cell clones in autoimmune diabetes: more lessons from the NOD mouse. Adv Immunol 87:123–162
6. Hultgren B, Huang X, Dybdal N, Stewart TA (1996) Genetic absence of γ-interferon delays but does not prevent diabetes in NOD mice. Diabetes 45:812–817
7. Serreze DV, Chapman HD, Post CM, Johnson EA, Suarez-Pinzon WL, Rabinovitch A (2001) Th1 to Th2 cytokine shifts in nonobese diabetic mice: sometimes an outcome, rather than the cause, of diabetes resistance elicited by immunostimulation. J Immunol 166:1352–1359
8. Trembleau S, Penna G, Gregori S et al (1999) Pancreas-infiltrating Th1 cells and diabetes develop in IL-12-deficient nonobese diabetic mice. J Immunol 163:2960–2968
9. Serreze DV, Post CM, Chapman HD, Johnson EA, Lu B, Rothman PB (2000) Interferon-gamma receptor signaling is dispensable in the development of autoimmune type 1 diabetes in NOD mice. Diabetes 49:2007–2011

10. Kanagawa O, Xu G, Tevaarwerk A, Vaupel BA (2000) Protection of nonobese diabetic mice from diabetes by gene(s) closely linked to IFN-gamma receptor loci. J Immunol 164:3919–3923
11. Komiyama Y, Nakae S, Matsuki T et al (2006) IL-17 plays an important role in the development of experimental autoimmune encephalomyelitis. J Immunol 177:566–573
12. Nakae S, Nambu A, Sudo K, Iwakura Y (2003) Suppression of immune induction of collagen-induced arthritis in IL-17-deficient mice. J Immunol 171:6173–6177
13. Veldhoen M, Hocking RJ, Flavell RA, Stockinger B (2006) Signals mediated by transforming growth factor-beta initiate autoimmune encephalomyelitis, but chronic inflammation is needed to sustain disease. Nat Immunol 7:1151–1156
14. Sutton C, Brereton C, Keogh B, Mills KH, Lavelle EC (2006) A crucial role for interleukin (IL)-1 in the induction of IL-17-producing T cells that mediate autoimmune encephalomyelitis. J Exp Med 203:1685–1691
15. Nakae S, Saijo S, Horai R, Sudo K, Mori S, Iwakura Y (2003) IL-17 production from activated T cells is required for the spontaneous development of destructive arthritis in mice deficient in IL-1 receptor antagonist. Proc Natl Acad Sci U S A 100:5986–5990
16. Horie I, Abiru N, Nagayama Y et al (2009) T helper type 17 immune response plays an indispensable role for development of iodine-induced autoimmune thyroiditis in nonobese diabetic-H2h4 mice. Endocrinology 150:5135–5142
17. Haskins K, Cooke A (2011) CD4 T cells and their antigens in the pathogenesis of autoimmune diabetes. Curr Opin Immunol 23:739–745
18. Jain R, Tartar DM, Gregg RK et al (2008) Innocuous IFNgamma induced by adjuvant-free antigen restores normoglycemia in NOD mice through inhibition of IL-17 production. J Exp Med 205:207–218
19. Emamaullee JA, Davis J, Merani S et al (2009) Inhibition of Th17 cells regulates autoimmune diabetes in NOD mice. Diabetes 58:1302–1311
20. Joseph J, Bittner S, Kaiser FM, Wiendl H, Kissler S (2012) IL-17 silencing does not protect nonobese diabetic mice from autoimmune diabetes. J Immunol 188:216–221
21. Zhou L, Chong MM, Littman DR (2009) Plasticity of CD4+ T cell lineage differentiation. Immunity 30:646–655
22. Lee YK, Turner H, Maynard CL et al (2009) Late developmental plasticity in the T helper 17 lineage. Immunity 30:92–107
23. Martin-Orozco N, Chung Y, Chang SH, Wang YH, Dong C (2009) Th17 cells promote pancreatic inflammation but only induce diabetes efficiently in lymphopenic hosts after conversion into Th1 cells. Eur J Immunol 39:216–224
24. Bending D, de la Pena H, Veldhoen M et al (2009) Highly purified Th17 cells from BDC2.5NOD mice convert into Th1-like cells in NOD/SCID recipient mice. J Clin Invest 119:565–572
25. Nakae S, Komiyama Y, Nambu A et al (2002) Antigen-specific T cell sensitization is impaired in IL-17-deficient mice, causing suppression of allergic cellular and humoral responses. Immunity 17:375–387
26. Serreze DV, Chapman HD, Varnum DS et al (1996) B lymphocytes are essential for the initiation of T cell-mediated autoimmune diabetes: analysis of a new "speed-congenic" stock of NOD.Ig μ null mice. J Exp Med 184:2049–2053
27. Yu L, Robles DT, Abiru N et al (2000) Early expression of antiinsulin autoantibodies of humans and the NOD mouse: evidence for early determination of subsequent diabetes. Proc Natl Acad Sci U S A 97:1701–1706
28. Wang B, André I, Gonzalez A et al (1997) Interferon-gamma impacts at multiple points during the progression of autoimmune diabetes. Proc Natl Acad Sci U S A 94:13844–13849
29. King C, Ilic A, Koelsch K, Sarvetnick N (2004) Homeostatic expansion of T cells during immune insufficiency generates autoimmunity. Cell 117:265–277
30. Liu SM, Lee DH, Sullivan JM et al (2011) Differential IL-21 signaling in APCs leads to disparate Th17 differentiation in diabetes-susceptible NOD and diabetes-resistant NOD.Idd3 mice. J Clin Invest 121:4303–4310
31. Dardenne M, Lepault F, Bendelac A, Bach JF (1989) Acceleration of the onset of diabetes in NOD mice by thymectomy at weaning. Eur J Immunol 19:889–895
32. Harada M, Makino S (1982) Promotion of spontaneous diabetes in nonobese diabetes-prone mice by cyclophosphamide. Diabetologia 27:604–606
33. Sadelain MW, Qin H-Y, Lauzon J, Singh B (1990) Prevention of type I diabetes in NOD mice by adjuvant immunotherapy. Diabetes 39:583–589
34. Mori Y, Kato T, Kodaka T, Kanagawa EM, Hori S, Kanagawa O (2008) Protection of IFN-gamma signaling-deficient NOD mice from diabetes by cyclophosphamide. Int Immunol 20:1231–1237
35. Mori Y, Kodaka T, Kato T, Kanagawa EM, Kanagawa O (2009) Critical role of IFN-gamma in CFA-mediated protection of NOD mice from diabetes development. Int Immunol 21:1291–1299
36. Zhu J, Paul WE (2010) Heterogeneity and plasticity of T helper cells. Cell Res 20:4–12
37. Bertin-Maghit S, Pang D, O'Sullivan B et al (2011) Interleukin-1beta produced in response to islet autoantigen presentation differentiates T-helper 17 cells at the expense of regulatory T cells: implications for the timing of tolerizing immunotherapy. Diabetes 60:248–257
38. Lexberg MH, Taubner A, Albrecht I et al (2010) IFN-gamma and IL-12 synergize to convert in vivo generated Th17 into Th1/Th17 cells. Eur J Immunol 40:3017–3027
39. Bending D, Newland S, Krejci A, Phillips JM, Bray S, Cooke A (2011) Epigenetic changes at Il12rb2 and Tbx21 in relation to plasticity behavior of Th17 cells. J Immunol 186:3373–3382
40. Nurieva R, Yang XO, Chung Y, Dong C (2009) Cutting edge: in vitro generated Th17 cells maintain their cytokine expression program in normal but not lymphopenic hosts. J Immunol 182:2565–2568
41. Honkanen J, Nieminen JK, Gao R et al (2010) IL-17 immunity in human type 1 diabetes. J Immunol 185:1959–1967
42. Marwaha AK, Crome SQ, Panagiotopoulos C et al (2010) Cutting edge: increased IL-17-secreting T cells in children with new-onset type 1 diabetes. J Immunol 185:3814–3818

Clinical & Experimental Immunology
The Journal of Translational Immunology

Clinical and Experimental Immunology ORIGINAL ARTICLE doi:10.1111/cei.12134

Genetic deletion of granzyme B does not confer resistance to the development of spontaneous diabetes in non-obese diabetic mice

M. Kobayashi,* C. Kaneko-Koike,† N. Abiru,* T. Uchida,† S. Akazawa,* K. Nakamura,* G. Kuriya,* T. Satoh,* H. Ida,** E. Kawasaki,‡ H. Yamasaki,¶ Y. Nagayama,§ H. Sasaki† and A. Kawakami*

*Department of Endocrinology and Metabolism, Unit of Translational Medicine, Graduate School of Biomedical Science, Departments of †Hospital Pharmacy, ‡Metabolism/Diabetes and Clinical Nutrition and §Molecular Medicine, ¶Center for Health and Communicating Medicine, Nagasaki University, Nagasaki, and **Division of Respirology, Neurology and Rheumatology, Department of Medicine, Kurume University, Kurume, Fukuoka, Japan

Accepted for publication 6 May 2013
Correspondence: N. Abiru, Department of Endocrinology and Metabolism, Unit of Translational Medicine, Graduate School of Biomedical Science, Nagasaki University, 1-7-1 Sakamoto, Nagasaki 852-8501, Japan.
E-mail: abirun@nagasaki-u.ac.jp

Masakazu Kobayashi and Chieko Kaneko-Koike contributed equally to this study.

Summary

Granzyme B (GzmB) and perforin are proteins, secreted mainly by natural killer cells and cytotoxic T lymphocytes that are largely responsible for the induction of apoptosis in target cells. Because type 1 diabetes results from the selective destruction of β cells and perforin deficiency effectively reduces diabetes in non-obese diabetic (NOD) mice, it can be deduced that β cell apoptosis involves the GzmB/perforin pathway. However, the relevance of GzmB remains totally unknown in non-obese diabetic (NOD) mice. In this study we have focused on GzmB and examined the consequence of GzmB deficiency in NOD mice. We found that *NOD.GzmB*$^{-/-}$ mice developed diabetes spontaneously with kinetics similar to those of wild-type NOD (*wt-NOD*) mice. Adoptive transfer study with regulatory T cell (T_{reg})-depleted splenocytes (SPCs) into NOD-SCID mice or *in-vivo* T_{reg} depletion by anti-CD25 antibody at 4 weeks of age comparably induced the rapid progression of diabetes in the *NOD.GzmB*$^{-/-}$ mice and *wt-NOD* mice. Expression of GzmA and Fas was enhanced in the islets from pre-diabetic *NOD.GzmB*$^{-/-}$ mice. In contrast to spontaneous diabetes, GzmB deficiency suppressed the development of cyclophosphamide-promoted diabetes in male NOD mice. Cyclophosphamide treatment led to a significantly lower percentage of apoptotic $CD4^+$, $CD8^+$ and $CD4^+CD25^+$ T cells in SPCs from *NOD.GzmB*$^{-/-}$ mice than those from *wt-NOD* mice. In conclusion, GzmB, in contrast to perforin, is not essentially involved in the effector mechanisms for β cell destruction in NOD mice.

Keywords: apoptosis, NOD mice, transgenic/knock-out mice, type 1 diabetes

Introduction

Type 1 diabetes is characterized by progressive autoimmune destruction of islet β cells with a long prodromal phase [1]. The hallmark of immune-mediated diabetes is T cell-mediated destruction of the insulin-producing β cells in the islets in both humans and the non-obese diabetic (NOD) mouse model of type 1 diabetes [2]. The precise mechanisms of β cell destruction leading to diabetes remain unclear. Many molecules, including Fas ligand (FasL) and cytokines, such as interleukin (IL)-1β, tumour necrosis factor (TNF)-α and interferon (IFN)-γ, cause release of other cytokine mediators that have the potential to damage the β cells [3]. Granzyme B (GzmB) and perforin have been shown to induce cytotoxic T lymphocyte (CTL)-mediated target cell apoptosis [4,5]. Perforin is involved in pore formation across the membranes via a Ca^{2+}-dependent mechanism. This pore enables the entry of serine protease granzymes into the cell, causing the cleavage and activation of several targets, such as effector caspases and the BH3-only protein Bid [6]. Some researchers believe that perforin/granzyme cause the initial β cell insult in diabetes, because spontaneous diabetes and cyclophosphamide (CYP)-induced diabetes are suppressed in perforin knock-out NOD mice [7]. However, the relevance of GzmB remains totally unknown in the pathogenesis of type 1 diabetes.

This study was therefore conducted to investigate the role of GzmB in the pathogenesis of a spontaneous type 1 diabetes model studying the NOD mouse whose disease pathogenesis, specifically in relation to autoimmune-mediated β cell destruction, is most probably similar to that in human type 1 diabetes.

© 2013 British Society for Immunology,

Table 1. Polymorphic markers at known non-obese diabetic (NOD) diabetes susceptibility (idd) loci and genotyping marker of granzyme B (GzmB).

Idd loci/chromozome	Satellite marker	Primer sequence
Idd1/chr17	D17*Mit34*	5′-TGTTGGAGCTGAATACACGC-3′
		5′-GGTCCTTGTTTATTCCCAGTACC-3′
Idd2/chr9	D9*Mit205*	5′AATAGCCTACTCTGGATTCACAGG-3′
		5′-TACCTTCTCCTCTTTGGTTTTTG 3′
Idd3/chr3	D3*Mit95*	5′-CTAAAAGCACTAGCAAAGAAAATCA-3′
		5′-CCTCCACACACATGTCCTTG-3′
Idd4/chr11	D17*Mit34*	5′-ATGAGACCATGCTCCTCCAC-3′
		5′-TTGTCCTCTGACCTTCACACC-3′
Idd5/chr1	D1*Mit18*	5′-TCTGGTTCCAGGCTTGATTC-3′
		5′-TCACAAGTGAGGCTCCAGG-3′
Idd6/chr6	D6*Mit339*	5′-ATATCGATTGGCTTCTAAATGTCA-3′
		5′-GCAGGTTGTCCTCTCACCTC-3′
Idd7/chr7	D7*Mit20*	5′-GTGTAGCAATGGTGTCGGTG-3′
		5′-AAGCCTGCCTCCAGATGTAA-3′
Idd8&12/chr14	D14*Mit222*	5′-GGTCAGTGAGAAGCCCTGTC-3′
		5′-GTCTAACTGCTTTTTTGTGGGG-3′
Idd9&11/chr4	D4*Mit59*	5′-AGAGTTTGGTCTCTTCCCCTG-3′
		5′-TATCCAACACATTTATGTCTGCG-3′
Idd10/chr3	D3*Mit103*	5′-CCAGGGGTGGTGGTCTTAC-3′
		5′-TGTCAGGTGCCCAGGTCT-3′
Idd13/chr2	D2*Mit17*	5′-AGGCAATTACAAGGCCTGG-3′
		5′-CACCCATCTCCCTCAGTCAT-3′
Idd14/chr13	D13*Mit61*	5′-TGCTCCAATACAACAAGGTCC-3′
		5′-CCAGCCAAGGTGTGTTGAC-3′
GzmB/chr14		5′GGACAAAGGCAGGTGAGTAAGCAA-3′
		5′-TTGATGACTGAGTTTGGGGTGAGG-3′
Mutated GzmB	*Neo 0013/0014*	5′-CTTGGGTGGAGAGGCTATTC-3′
		5′-AGGTGAGATGACAGGAGATC-3′

Materials and methods

Mice

Female NOD mice and NOD-severe combined immunodeficient (SCID) mice were purchased from Clea Japan (Tokyo, Japan), and C57BL/6-GzmB-deficient mice (B6·129S2-Gzmb^{tm1Ley}, stock number 002248) were purchased from the Jackson Laboratory (Bar Harbor, ME, USA); all animals were maintained in the Laboratory Animal Center for Biomedical Research at Nagasaki University under specific pathogen-free conditions. All animal experiments described in this study were approved by the institutional animal experimentation committee and were conducted in accordance with the Guidelines for Animal Experimentation.

Establishment of granzyme B-deficient NOD mice

We have established NOD mice with the GzmB gene deleted by back-crossing C57BL/6-GzmB-deficient mice (B6·129S2-Gzmb^{tm1Ley}) with NOD mice. The targeted allele was introgressed into the NOD background using a marker-assisted 'speed congenic' breeding approach, wherein backcross segregants were fixed for homozygosity for NOD alleles at NOD/B6/129 polymorphic markers at known NOD diabetes susceptibility (idd) loci (Table 1). We determined the GzmB knock-out gene utilizing polymerase chain reaction (PCR) amplification to detect the primer's neomycin sequence (Table 1) in the disrupted knock-out gene. We screened an additional four markers on chromosome 14 flanking the GzmB mutation to define the size of the congenic interval. N4 mice were NOD-derived at all markers (iddm 1–14) tested across the genome, except for a congenic interval of less than 5 cM flanking the GzmB-targeted mutation on chromosome 14, thereby excluding the possibility that the presence of the 129S2 genome could contribute resistance at the *Idd8&12* locus on that chromosome. Homozygous GzmB-deficient NOD background mice (*NOD.GzmB*$^{-/-}$) were produced by intercrossing of heterozygotes at N11, and a permanent line of *NOD.GzmB*$^{-/-}$ and wild-type (*wt-NOD*) mice were established at N11.

Monitoring for spontaneous diabetes and cyclophosphamide-promoted diabetes

Blood glucose levels were monitored using One-touch Ultra (Johnson & Johnson, Tokyo, Japan) every other week starting at 12 weeks of age for spontaneous diabetes. For CYP-

promoted diabetes, 200 mg/kg of CYP (Sigma-Aldrich KK, Tokyo, Japan) was injected intraperitoneally (i.p.) at 9 and 11 weeks of age, as described previously [7,8]. Blood glucose levels were monitored at 10 weeks of age and three times a week, starting at 11 weeks of age.

Mice with blood glucose levels above 250 mg/dl for two consecutive measurements were considered diabetic.

Histology

Pancreatic sections were analysed histologically by fixing tissues in 10% formalin and staining the paraffin-embedded samples with haematoxylin and eosin. A minimum of 30 islets from each mouse were observed microscopically by two different observers for the presence of insulitis, and the levels of insulitis were scored according to the following criteria: 0, no lymphocyte infiltration; 1, islets with lymphocyte infiltration in less than 25% of the area; 2, 25–50% of the islet infiltrated; 3, 50–75% of the islet infiltrated; and 4, more than 75% infiltrated or small retracted islets.

Adoptive transfer experiments

Non-diabetic 12–14-week-old donor mice (*NOD.GzmB*$^{-/-}$ or wt-NOD) were killed and their spleens were harvested under sterile conditions. CD25$^+$ T cells were depleted from 12–14-week-old donor mice splenocytes using a CD25 MicroBead Kit (Miltenyi Biotec, Auburn, CA, USA) by Auto-MACS, according to the manufacturer's protocol. CD25$^+$ T cell-depleted splenocytes ($1{\cdot}5 \times 10^7$ per mouse) were injected i.p. into 8–12-week-old NOD-SCID recipient mice. The mice were monitored for blood glucose biweekly after adoptive transfer.

In-vivo regulatory T cell (T_{reg})-depletion by anti-CD25 antibody (PC61)

Anti-CD25 monoclonal antibody was purified from ascites of mice injected i.p. with hybridoma PC61 using a HiTrapTM protein G HP column (Amersham, Piscataway, NJ, USA), as described previously [9]. Five hundred μg of anti-CD25 antibody was injected i.p. at 4 weeks and the blood glucose levels were monitored every week, starting at 10 weeks of age.

Real-time quantitative polymerase chain reaction (PCR)

Islets were isolated from 20-week-old female mice by pancreatic digestion with collagenase (Wako Pure Chemical Industries Ltd, Tokyo, Japan). Islets were purified by Histopaque (Sigma-Aldrich, Tokyo, Japan) density gradient centrifugation. Isolated islets were stored at –80°C until use. Total RNA was extracted from mice islets. cDNA synthesis was performed using primers using the SuperScript III First-strand Synthesis System for reverse transcription (RT)–PCR (Invitrogen, Carlsbad, CA, USA). cDNAs were used as templates in SYBR green real-time PCR assays on a LightCycler (Roche Diagnostics, Tokyo, Japan). The primers used in the PCR reaction for GzmB, granzyme A (GzmA), granzyme C (GzmC), Fas and perforin were obtained from SA Biosciences. Sample data were analysed according to the comparative cycle threshold method and were normalized by stable reference genes of β-actin and glyceraldehyde 3-phosphate dehydrogenase (GAPDH) selected by geNorm visual basic application (VBA) applet among three housekeeping genes, including β-actin, GAPDH and 18S. All results were expressed as a percentage of the value in control extracts.

Apoptosis

Staining for apoptosis was conducted on single-cell suspensions of splenocytes (SPCs). A total of 1×10^6 SPCs were incubated for 15 min at room temperature with 5 μl of annexin V-fluorescein isothiocyanate (FITC), 1 μl of anti-CD4-allophycocyanin (APC) monoclonal antibody (mAb), 1 μl of anti-CD8-APC mAb, 1 μl of anti-CD25-phycoerythin (PE) mAb and 5 μl of propidium iodide (PI). All fluorescein-labelled antibodies were purchased from BD Pharmingen. The result was calculated based on the differences in annexin V percentage between CYP-treated cells and non-CYP-treated cells. All cells were analysed on a FACSCanto II flow cytometry system using FACS Diva software (BD Biosciences, Tokyo, Japan).

Statistics analysis

Group differences were analysed by the Mann–Whitney *U*-test and Student's *t*-test. Differences between Kaplan–Meier survival curves were estimated by the log-rank test, with the use of DR SPSS version 2 for Windows software (SPSS, Inc., Chicago, IL, USA). *P*-values less than 0·05 were considered statistically significant. Insulitis levels were analysed by Ridit analysis, and levels of *t* higher than 1·96 or lower than –1·96 were considered statistically significant.

Results

GzmB deletion did not affect the spontaneous development of diabetes and insulitis

NOD mice develop diabetes after 12 weeks of age, with a higher incidence in females than males [10]. In our colony, 75–85% of female and 10–20% of male NOD mice develop diabetes by age 48 weeks. Using speed congenic techniques with diabetogenic loci (iddm 1–14), we have established

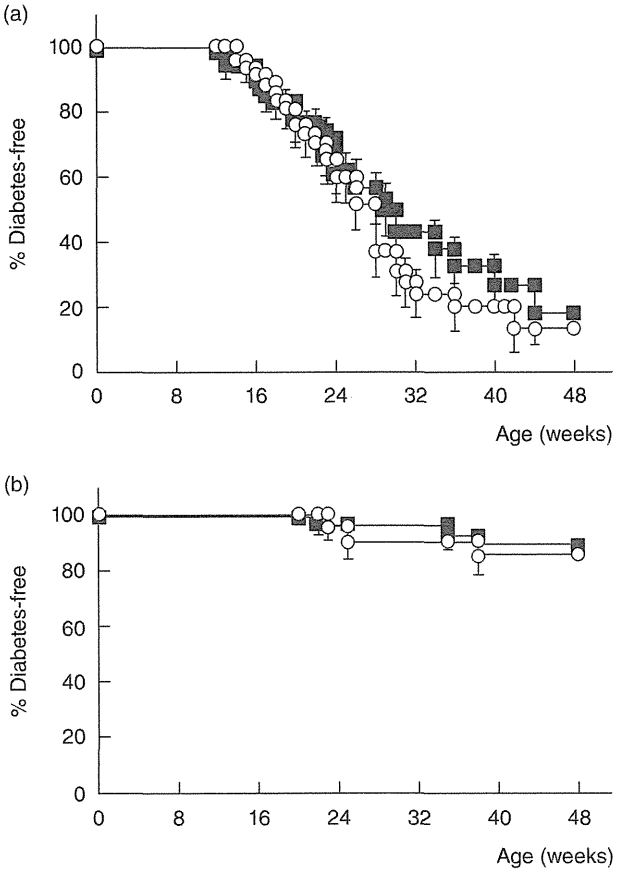

Fig. 1. Life-table analysis for the development of spontaneous diabetes. Blood glucose levels were monitored every week starting at 12 weeks and every other week from 20 weeks. (a) Female mice. Squares: wild-type non-obese diabetic (*wt-NOD*) ($n = 47$). Open circles: *NOD*.granzyme B $(GzmB)^{-/-}$ ($n = 44$). (b) Male mice. Squares: wt-NOD ($n = 27$), open circles: $NOD.GzmB^{-/-}$ ($n = 21$).

NOD mice with GzmB deleted. In the established *wt-NOD* mice, 82% (39 of 47) of female mice and 11% (three of 27) of male mice developed diabetes by age 48 weeks. This implied that 10–11 back-crossed mice become NOD-background from a C57BL/6-background. Among female mice, $NOD.GzmB^{-/-}$ mice became diabetic starting at 14 weeks of age, and *wt-NOD* mice became diabetic starting at 12 weeks of age. The incidence of spontaneous diabetes was essentially identical between these two groups ($P = 0{\cdot}46$) (Fig. 1a). In male mice, $NOD.GzmB^{-/-}$ mice became diabetic starting at 23 weeks of age, and *wt-NOD* mice became diabetic starting at 22 weeks of age. As in female mice, the incidence of spontaneous diabetes was essentially identical between these groups ($P = 0{\cdot}91$) (Fig. 1b). We next compared the levels of the insulitis between female $NOD.GzmB^{-/-}$ and *wt-NOD* mice at 12 weeks of age and found that there were no significant differences between both groups (Ridit score, $T = 1{\cdot}27$) (Fig. 2). These results are consistent with the report by Thomas *et al.* [11].

GzmB deficiency did not affect the adoptively transferred diabetes with T_{reg}-depleted SPCs or *in-vivo* T_{reg}-depletion in the NOD mice

Recent reports indicate that GzmB might be a key molecule for the suppressive function in $CD4^+CD25^+$ T_{regs} as well as the function of effector T cells (T_{effs}) for target cell destruction [12]. To investigate the relevance of GzmB in the function of T_{effs} and T_{regs}, we performed an adoptive transfer study involving the transfer of T_{reg}-depleted SPCs and *in-vivo* T_{reg}-depletion in $NOD.GzmB^{-/-}$ mice or *wt-NOD* mice. The NOD-SCID mice transferred with T_{reg}-depleted SPCs from both groups became diabetic starting at 3 weeks of transfer. The incidence of diabetes was 87·5% in the $NOD.GzmB^{-/-}$ mice and 75% in the *wt-NOD* mice at 10 weeks after transfer ($P > 0{\cdot}05$) (Fig. 3a). We also found that T_{reg} depletion by anti-CD25 antibody at 4 weeks of age accelerated diabetes in the $NOD.GzmB^{-/-}$ mice as well as in *wt-NOD* mice and that the course of disease development did not show any significant difference between these groups (Fig. 3b). Taken together, GzmB does not affect the disease pathogenesis in relation not only to β cell destruction by T_{effs}, but also the suppressive function of T_{regs} in NOD mice.

Expression of GzmA and Fas was enhanced in the islets from pre-diabetic $NOD.GzmB^{-/-}$ mice

We evaluated the expression of GzmB in the islets of pre-diabetic $NOD.GzmB^{-/-}$ mice or *wt-NOD* mice. As expected, GzmB was expressed in the islets from pre-diabetic *wt-NOD* mice but not in those from $NOD.GzmB^{-/-}$ mice or NOD-*SCID* mice (Fig. 4). However, there was no significant alteration in the expression levels of GzmB in islets from 12-week-old *wt-NOD* mice and 20-week-old pre-diabetic

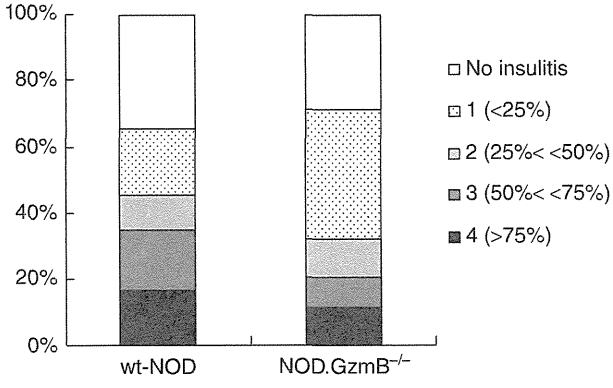

Fig. 2. Histological analysis for insulitis. Levels of insulitis in wild-type non-obese diabetic (*wt-NOD*) mice ($n = 5$) and *NOD*.granzyme B $(GzmB)^{-/-}$ mice ($n = 5$) at 12 weeks of age. A level of $T > 1{\cdot}96$ determined by Ridit analysis was regarded as significant. No significant difference was found between the two groups at 12 weeks of age ($T = 1{\cdot}27$).

© 2013 British Society for Immunology,

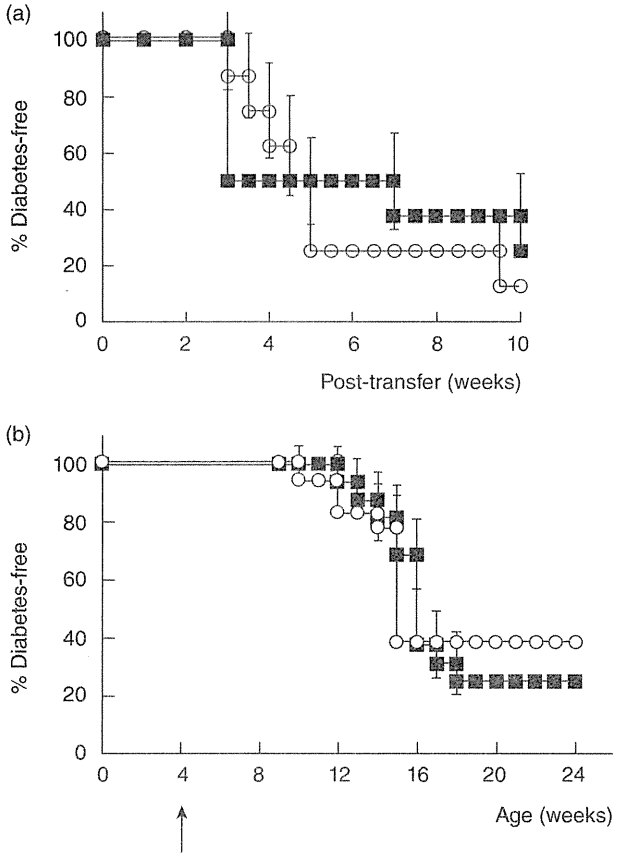

Fig. 3. Adoptive transfer study and the development of diabetes following injection of PC61. (a) $CD25^+$-depleted splenocytes (2×10^7) from non-obese diabetic.granzyme B $(NOD.GzmB)^{-/-}$ ($n = 8$ open circle) and wild-type (*wt*)-*NOD* ($n = 8$ square) mice were transferred into *NOD*-SCID mice. (b) Diabetes-free ratios in *in-vivo* regulatory T cell (T_{reg})-depleted *NOD*.$GzmB^{-/-}$ ($n = 18$ open circle) and *wt-NOD* ($n = 16$ square) following injection of PC61 at 4 weeks of age.

mice. We also investigated the mRNA expression of other apoptosis-associated molecules, including GzmA, GzmC, perforin and Fas in the pre-diabetic *wt-NOD* mice and *NOD.GzmB*$^{-/-}$ mice, to evaluate the mechanism of diabetic induction in *NOD.GzmB*$^{-/-}$mice. Expressions of GzmA and Fas, but not GzmC, were significantly higher in *NOD.GzmB*$^{-/-}$ mice than those in *wt-NOD* mice (GzmA: $P < 0{\cdot}01$, Fas: $P < 0{\cdot}01$). No significant difference in the expression levels of perforin was observed between these groups.

GzmB deficiency suppressed the development of CYP-promoted diabetes in male NOD mice

Injection of CYP induces a rapid rise and high percentage of diabetes in NOD mice of both sexes [8]. CYP was injected twice into *wt-NOD* mice or *NOD.GzmB*$^{-/-}$ mice at 9 and 11 weeks of age. Some of the *wt-NOD* mice developed diabetes on days 9–14 before the second injection, but most became diabetic only after the second injection of CYP between days 21 and 25, with incidences of 60% for female mice and 80% for male mice at 60 days after the first injection. However, in *NOD.GzmB*$^{-/-}$ mice diabetes occurred mainly between days 14 and 25, and the incidence was reduced to 40% for female mice ($P = 0{\cdot}32$) or 30% for male mice compared to those of *wt-NOD* mice ($P = 0{\cdot}0031$) (Fig. 5a,b).

T cells from CYP-treated $GzmB^{-/-}$ mice display reduced apoptosis

Previous study has shown that *in-vivo* blockade of the Fas–Fas ligand pathway also inhibits CYP-promoted diabetes. Interestingly, this protective effect was not due to suppression of β cell apoptosis, but rather to the apoptosis resistance in both $CD4^+$ and $CD8^+$ T cells by the CYP [13]. To verify whether or not NOD T cells from CYP-treated mice showed a comparable functional impairment, we isolated $CD4^+$, $CD8^+$ and $CD4^+CD25^+$ T cells 48 h after CYP dosing and compared them with those cells from untreated littermate controls. Analysis of the proportions of apoptotic cells stained by annexin V after CYP treatment showed a significantly greater percentage of apoptotic $CD4^+$, $CD8^+$ or $CD4^+CD25^+$ T cells in *wt-NOD* mice than in *NOD.GzmB*$^{-/-}$ mice ($CD4^+$: $23{\cdot}82 \pm 3{\cdot}82\%$ *versus* $4{\cdot}36 \pm 1{\cdot}99\%$, $P < 0{\cdot}01$; $CD8^+$: $11{\cdot}64 \pm 6{\cdot}23\%$ *versus* $1{\cdot}94 \pm 5{\cdot}32\%$, $P < 0{\cdot}05$; $CD4^+CD25^+$: $7{\cdot}10 \pm 4{\cdot}66\%$ *versus* $0{\cdot}32 \pm 0{\cdot}35\%$, $P < 0{\cdot}05$) (Fig. 6).

Discussion

Perforin/granzymes cause the initial β cell insult in diabetes, as demonstrated by the fact that spontaneous diabetes and

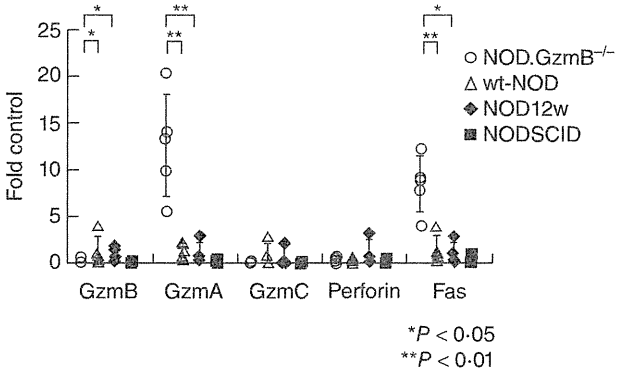

Fig. 4. Real-time reverse transcription–polymerase chain reaction (RT–PCR) analysis of islets in pre-diabetic mice. Real-time RT–PCR of mouse islets at 20 weeks age in wild-type non-obese diabetic (*wt-NOD*) mice, *NOD*.granzyme B $(GzmB)^{-/-}$ mice and NOD-*SCID* mice. Values are the means ± standard error and are expressed as a percentage of the mRNA levels in islets isolated from control 12-week-old *wt-NOD* mice at the same time. *wt-NOD* ($n = 5$), *NOD.GzmB*$^{-/-}$ ($n = 5$).

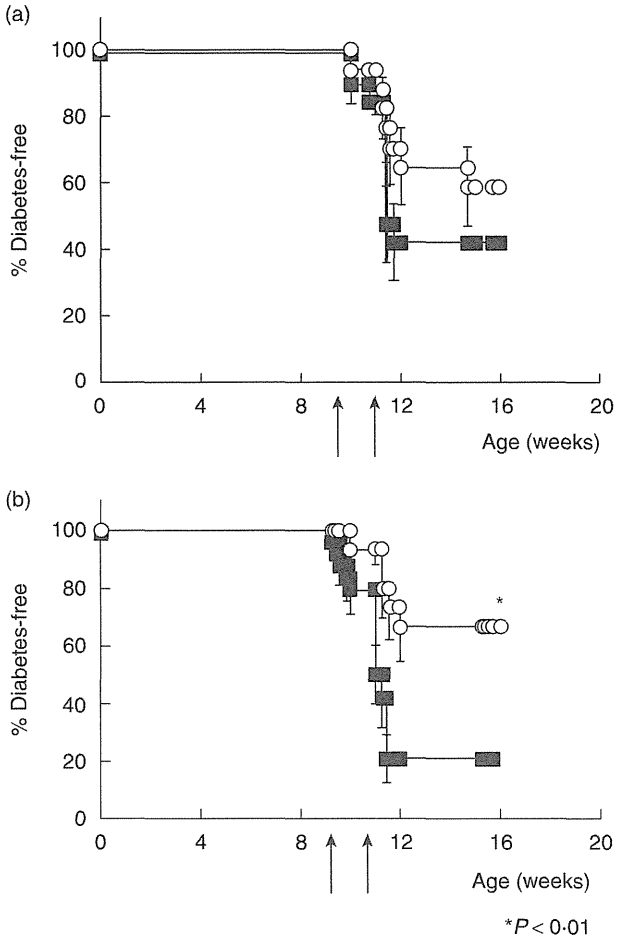

Fig. 5. Life-table analysis for the development of cyclophosphamide (CYP)-promoted diabetes; 200 mg/kg of CYP was injected intraperitoneally (i.p.) at 9 and 11 weeks of age. Blood glucose levels were monitored three times a week starting at 11 weeks of age. (a) Female mice. Squares: wild-type non-obese diabetic (*wt-NOD*) ($n = 19$). Open circles: *NOD*.granzyme B (*GzmB*)$^{-/-}$ ($n = 17$). (b) Male mice. Squares: *wt-NOD* ($n = 24$). Open circles: *NOD.GzmB*$^{-/-}$ ($n = 15$).

CYP-induced diabetes were suppressed in perforin knock-out NOD mice [7] while, in a model of viral infection, it has been reported that perforin and granzymes have distinct roles in defensive immunity and immunopathology [14]. We therefore investigated the significance of GzmB on β cell destruction using GzmB-deficient NOD mice. In contrast to perforin-deficient NOD mice, GzmB-deficient NOD mice did not show reduced spontaneous diabetes, consistent with a recent report by Thomas *et al.* [11].

The question then arises as to why GzmB-deficient NOD mice exhibit the distinct phenotype from perforin-deficient NOD mice. In particular, GzmB, but not perforin, is reported to affect not only effector function of CTL but also suppressive function in T_{regs} [12]. One possible explanation for the dissociation between GzmB and perforin is that a reduced suppressive T_{reg} function in GzmB-deficient NOD mice might modify the phenotype of diabetes development.

To evaluate the influence of T_{regs} in our study, we performed an adoptive transfer study with T_{reg}-depleted SPCs to NOD-SCID mice and found that the cells derived from *NOD.GzmB*$^{-/-}$ mice induced rapid progression of diabetes, a result similar to that of *wt-NOD* mice. We also found that T_{reg} depletion accelerated diabetes in the *NOD.GzmB*$^{-/-}$ mice as well as *wt-NOD* mice. These results emphasized the conclusion that GzmB is not essentially involved in the effector mechanisms for β cell destruction and might not affect the suppressive function in T_{regs} in the NOD mouse.

Another possible reason for the dissociation is that gene targeting to GzmB, but not to perforin, causes the compensating mechanisms to induce β cell apoptosis when the gene is missing. Of the granzyme family of serine proteases,

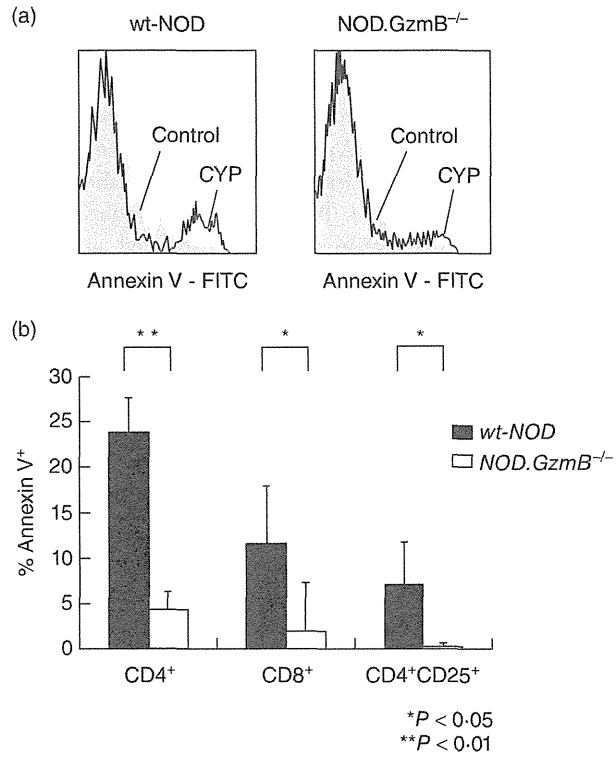

Fig. 6. Effects of cyclophosphamide (CYP) on the apoptosis of $CD4^+$ T cells, $CD8^+$ T cells and $CD4^+CD25^+$ T cells. Wild-type non-obese diabetic (*wt-NOD*) and *NOD*.granzyme B (*GzmB*)$^{-/-}$ mice were treated with 200 mg/kg CYP intraperitoneally (i.p.) at 8–10 weeks of age, and lymphocytes were prepared from spleens after 48 h for comparison with untreated littermate controls. $CD4^+$ lymphocytes, $CD8^+$ lymphocytes or $CD4^+25^+$ lymphocytes were stained with annexin V^{FITC} as described and analysed by flow cytometry. (a) Staining for apoptosis in $CD4^+$ T cells. Cells were gated initially on forward-scatter (FSC)/side-scatter (SSC) and CD4 expression, excluding all cells staining positive for PI. The percentage of annexin V^+ cells was determined as shown in the histogram overlays. (b) Graphs represent the arithmetic means and values for each individual mouse for the percentage of annexin V^+ $CD4^+$ T cells, annexin V^+ $CD8^+$ T cells and annexin V^+ $CD4^+CD25^+$ T cells in *wt-NOD* ($n = 5$ each), *NOD.GzmB*$^{-/-}$ ($n = 5$ each).

GzmA and GzmB are the most common in humans and mice. Other granzymes, including H, K and M in humans and C, D, E, F, G, K, L, M and N in mice, are less well characterized [15]. GzmB *in vitro* and GzmA *in-situ* analysis has shown that GzmB and GzmA play important roles in β cell destruction [16,17]. In a previous study using 8·3 T cell receptor (TCR)-transgenic NOD mice, perforin gene knock-out did not alter the development of diabetes [18]. The results of another study indicated that T cells from 8·3 TCR-transgenic NOD mice use both perforin and Fas pathways and that Fas compensates for the β cell killing only when perforin is missing [16]. In our *NOD.GzmB*$^{-/-}$ mice, the mRNA expressions of GzmA and Fas were up-regulated significantly compared to *wt-NOD* mice, indicating that there might be pathways to induce β cell death that can compensate fully for each other when GzmB, but not perforin, is removed in *wt-NOD* mice.

In contrast to spontaneous diabetes development, GzmB deficiency suppressed the incidence of CYP-promoted diabetes in NOD mice. In particular, male *NOD.GzmB*$^{-/-}$ mice were significantly less likely and female *NOD.GzmB*$^{-/-}$ mice showed a tendency to be less likely to develop diabetes compared to *wt-NOD* mice. Previous reports indicated that acceleration of diabetes by CYP was associated with a significant T cell depletion, especially with preferential reduction in CD4$^+$CD25$^+$forkhead box protein 3 (Foxp3)$^+$ T populations following injection [19,20]. In our study, both CD4$^+$, CD8$^+$ and CD4$^+$CD25$^+$ T cells from CYP-treated GzmB$^{-/-}$ mice displayed reduced apoptosis, suggesting that the suppression mechanism in *NOD.GzmB*$^{-/-}$ mice might be associated with apoptosis resistance of T cells rather than deficient effector mechanisms. As a result, GzmB deficiency confers resistance to CYP-promoted diabetes.

In conclusion, GzmB is not involved essentially in the effector mechanisms for β cell destruction in NOD mice. Instead, GzmB probably confers apoptosis resistance to T cells. It is possible that several compensation pathways are associated with β cell destruction in the GzmB-deficient NOD mice. If each single gene is not essential by itself, multiple gene knock-out models might be needed to evaluate the exact mechanism of β cell destruction in NOD mice.

Acknowledgements

This study was supported by research grants from the Japan Society for the Promotion of Science (#21591143, #23791036 and #21790874).

Disclosures

The authors have no financial conflicts of interest.

References

1 Eisenbarth GS. Type I diabetes mellitus. A chronic autoimmune disease. N Engl J Med 1986; **314**:1360–8.

2 Bottazzo GF, Dean BM, McNally JM, MacKay EH, Swift PG, Gamble DR. *In situ* characterization of autoimmune phenomena and expression of HLA molecules in the pancreas in diabetic insulitis. N Engl J Med 1985; **313**:353–60.

3 Kawasaki E, Abiru N, Eguchi K. Prevention of type 1 diabetes: from the view point of beta cell damage. Diabetes Res Clin Pract 2004; **66** (Suppl. 1):S27–32.

4 Lord SJ, Rajotte RV, Korbutt GS, Bleackley RC. Granzyme B: a natural born killer. Immunol Rev 2003; **193**:31–8.

5 Trapani JA, Sutton VR. Granzyme B: pro-apoptotic, antiviral and antitumor functions. Curr Opin Immunol 2003; **15**:533–43.

6 Pirot P, Cardozo AK, Eizirik DL. Mediators and mechanisms of pancreatic beta-cell death in type 1 diabetes. Arq Bras Endocrinol Metabol 2008; **52**:156–65.

7 Kagi D, Odermatt B, Seiler P, Zinkernagel RM, Mak TW, Hengartner H. Reduced incidence and delayed onset of diabetes in perforin-deficient nonobese diabetic mice. J Exp Med 1997; **186**:989–97.

8 Harada M, Makino S. Promotion of spontaneous diabetes in non-obese diabetes-prone mice by cyclophosphamide. Diabetologia 1984; **27**:604–6.

9 Fukushima K, Abiru N, Nagayama Y *et al.* Combined insulin B:9-23 self-peptide and polyinosinic–polycytidylic acid accelerate insulitis but inhibit development of diabetes by increasing the proportion of CD4+Foxp3+ regulatory T cells in the islets in non-obese diabetic mice. Biochem Biophys Res Commun 2008; **367**:719–24.

10 Makino S, Kunimoto K, Muraoka Y, Mizushima Y, Katagiri K, Tochino Y. Breeding of a non-obese, diabetic strain of mice. Jikken Dobutsu 1980; **29**:1–13.

11 Mollah ZU, Graham KL, Krishnamurthy B *et al.* Granzyme B is dispensable in the development of diabetes in non-obese diabetic mice. PLoS ONE 2012; **7**:e40357.

12 Gondek DC, Lu LF, Quezada SA, Sakaguchi S, Noelle RJ. Cutting edge: contact-mediated suppression by CD4+CD25+ regulatory cells involves a granzyme B-dependent, perforin-independent mechanism. J Immunol 2005; **174**:1783–6.

13 Mahiou J, Walter U, Lepault F, Godeau F, Bach JF, Chatenoud L. *In vivo* blockade of the Fas–Fas ligand pathway inhibits cyclophosphamide-induced diabetes in NOD mice. J Autoimmun 2001; **16**:431–40.

14 van Dommelen SL, Sumaria N, Schreiber RD, Scalzo AA, Smyth MJ, Degli-Esposti MA. Perforin and granzymes have distinct roles in defensive immunity and immunopathology. Immunity 2006; **25**:835–48.

15 Bolitho P, Voskoboinik I, Trapani JA, Smyth MJ. Apoptosis induced by the lymphocyte effector molecule perforin. Curr Opin Immunol 2007; **19**:339–47.

16 Estella E, McKenzie MD, Catterall T *et al.* Granzyme B-mediated death of pancreatic beta-cells requires the proapoptotic BH3-only molecule bid. Diabetes 2006; **55**:2212–9.

17 Mueller C, Held W, Imboden MA, Carnaud C. Accelerated beta-cell destruction in adoptively transferred autoimmune diabetes correlates with an increased expression of the genes coding for TNF-alpha and granzyme A in the intra-islet infiltrates. Diabetes 1995; **44**:112–7.

18 Amrani A, Verdaguer J, Anderson B, Utsugi T, Bou S, Santamaria P. Perforin-independent beta-cell destruction by diabetogenic

CD8(+) T lymphocytes in transgenic nonobese diabetic mice. J Clin Invest 1999; **103**:1201–9.

19 Gregori S, Giarratana N, Smiroldo S, Adorini L. Dynamics of pathogenic and suppressor T cells in autoimmune diabetes development. J Immunol 2003; **171**:4040–7.

20 Brode S, Raine T, Zaccone P, Cooke A. Cyclophosphamide-induced type-1 diabetes in the NOD mouse is associated with a reduction of CD4+CD25+Foxp3+ regulatory T cells. J Immunol 2006; **177**:6603–12.

Downloaded from ard.bmj.com on May 1, 2013 - Published by group.bmj.com

Phenotypic changes of lymphocyte in a patient with IgG4-related disease after corticosteroid therapy

Immunoglobulin G4-related disease (IgG4RD) is a novel clinical disease entity characterised by elevated serum IgG4 and tissue infiltration by IgG4-positive plasma cells.[1 2] Interleukin 4 (IL-4) and IL-10, which were detected with B cells in the salivary gland in this disease,[3] direct naive B cells to switch to IgG4 production.[4] B cells are therefore considered to be important for the pathogenesis of IgG4RD. However, the phenotype of B cells in patients with IgG4RD remains elusive. In this report we show the phenotypic changes of peripheral blood B cells in a patient with IgG4RD analysed by flow cytometry during treatment with a corticosteroid.

In January 2011 a 53-year-old man presented with symmetrical swelling of the lachrymal glands and a tumour located in the left junction of the renal pelvis and ureter, serum IgG4 >135 mg/dl and IgG4+/IgG+ cells >40% with significant invasion of lymphocytes and plasma cells, typical tissue fibrosis and sclerosis in the salivary gland. He was diagnosed with IgG4RD based on the guidelines for diagnosis.[5] Treatment with corticosteroid 40 mg (0.6 mg/kg) was started. One year later the bilateral renal pelvic tumour had disappeared and serum IgG (IgG4) decreased from 1692 (341) mg/dl to 969 (61.5) mg/dl despite tapering of the corticosteroid dose to 2 mg/day.

Meanwhile, before treatment, memory B cells (CD19 gated IgD-CD27 or CD27+ CD38-) and plasmablasts (CD19 gated $CD27^{high}CD38^{high}$ or IgD-$CD27^{high}$, $CD19^{low}CD38^{high}$) increased in a patient with IgG4RD compared with healthy donors in peripheral blood. Moreover, the expression levels of the costimulatory molecules CD80 were upregulated. Spleen tyrosine kinase (Syk) is a tyrosine kinase expressed in various immunocompetent cells including B cells. We have reported that the engagement of immune receptor phosphorylates Syk, resulting in proliferation and cytokine production on B cells.[6] It is noteworthy that Syk phosphorylation was also markedly increased in CD19 cells in the patient compared with those in healthy donors.

However, $CD27^{high}CD38^{high}$ plasmablasts in the patient decreased at 1 month and disappeared 6 months after treatment with corticosteroid, whereas the percentage of memory B cells almost did not change. Although he remained in low disease activity after tapering of the corticosteroid dose, the expression levels of CD80 and phospho-Syk on CD19 cells did not change until 1 year later (figure 1).

Taken together, although corticosteroid therapy effectively decreased peripheral plasmablasts, activated memory B cells were resistant to treatment in IgG4RD. These results are supported by those of Khosroshahi et al who demonstrated that B cell depletion therapy by rituximab was effective in some patients with IgG4RD refractory to corticosteroid.[7] The present data could therefore partly explain why IgG4RD is difficult to maintain in remission after reduction in the dose of corticosteroid. The results also indicate that the combined use of immunosuppressants, B cell-targeted therapies or Syk inhibitors may be considered for the treatment of IgG4RD, as shown in systemic lupus erythematosus, rheumatoid arthritis and idiopathic thrombocytopenic purpura.[8–10] However, further analysis of a large sample of patients is needed.

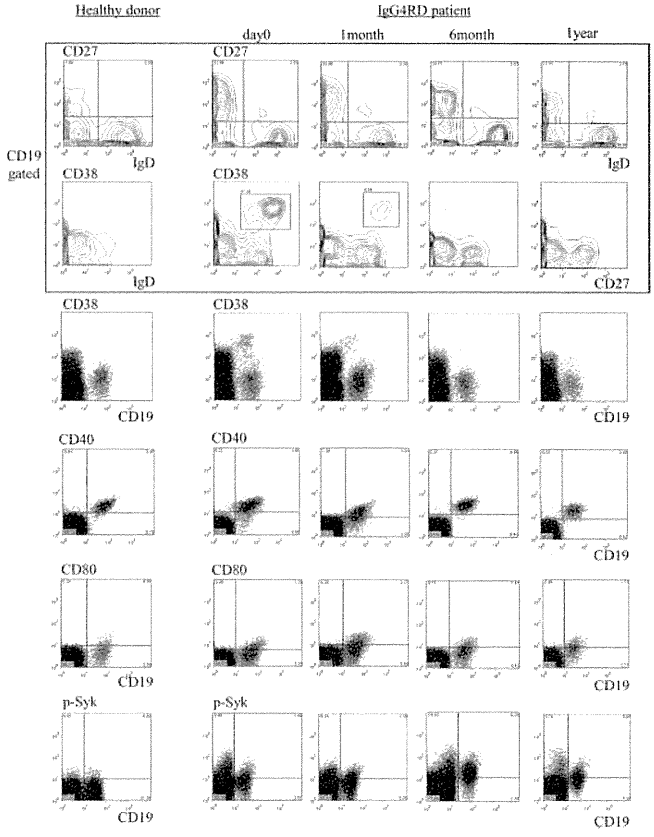

Figure 1 Phenotypic changes of B cells in a patient with IgG4-related disease before treatment, 1 month and 6 months after treatment with corticosteroid therapy. In the upper 10 contour line graphs, peripheral blood mononuclear cell (PBMCs) were gated on CD19-positive cells and further separated with CD27 and IgD, or CD38 and CD27. In the former, the left quadrant identified plasma cells (IgD-$CD27^{high}$) and class-switched memory B cells (IgD-CD27+). The right upper quadrant identified IgM memory B cells (IgD+CD27). The right lower quadrant identified naïve B cells (IgD+CD27+). In the latter, CD27−CD38 + identified naïve B cells, CD27+ CD38− identified memory B cells and $CD27^{high}CD38^{high}$ identified plasmablasts and plasma cells. In the lower four line graphs, PBMC were double-stained by CD19 (x-axis) and IgG isotype control, CD38, CD40, CD80 and Syk phosphorylation, respectively (y-axis). $CD19^{low}CD38^{high}$ identified plasmablasts and plasma cells.

Shigeru Iwata, Kazuyoshi Saito, Shintaro Hirata, Yoshiya Tanaka

The First Department of Internal Medicine, School of Medicine, University of Occupational and Environmental Health, Japan, Kitakyushu, Japan

Correspondence to Yoshiya Tanaka, University of Occupational and Environmental Health, Japan, The First Department of Internal Medicine, School of Medicine, 1-1 Iseigaoka, Yahatanishi Ward, Kitakyushu 807-8555, Fukuoka Prefecture, Japan; tanaka@med.uoeh-u.ac.jp

Acknowledgements The authors thank Ms T Adachi, Ms N Sakaguchi and Ms K Noda for the excellent technical assistance. This work was supported in part by a Research Grant-In-Aid for Scientific Research from the Ministry of Health, Labour and Welfare of Japan, the Ministry of Education, Culture, Sports, Science and Technology of Japan and the University of Occupational and Environmental Health, Japan.

Competing interests YT has received consulting fees, speaking fees and/or honoraria from Mitsubishi-Tanabe Pharma, Chugai Pharma, Eisai Pharma, Pfizer, Abbott Immunology Pharma, Daiichi-Sankyo, Janssen Pharma, Astra-Zeneca, Takeda Industrial Pharma, Astellas Pharma, Asahi-kasei Pharma and GlaxoSmithKline and has received research grant support from Mitsubishi-Tanabe Pharma, Bristol-Myers Squibb, Takeda Industrial Pharma, MSD, Astellas Pharma, Eisai Pharma, Chugai Pharma, Pfizer and Daiichi-Sankyo. The other authors declare no conflict of interest.

Downloaded from ard.bmj.com on May 1, 2013 - Published by group.bmj.com

Patient consent Obtained.

Ethics approval Ethics approval was obtained from the committee in University of Occupational and Environmental Health, Japan.

Provenance and peer review Not commissioned; externally peer reviewed.

Received 9 March 2012
Accepted 3 May 2012

Published Online First 11 July 2012

Ann Rheum Dis 2012;**71**:2058–2059.
doi:10.1136/annrheumdis-2012-201657

REFERENCES

1. **Hamano H,** Kawa S, Horiuchi A, *et al*. High serum IgG4 concentrations in patients with sclerosing pancreatitis. *N Engl J Med* 2001;**344**:732–8.
2. **Masaki Y,** Dong L, Kurose N, *et al*. Proposal for a new clinical entity, IgG4-positive multiorgan lymphoproliferative syndrome: analysis of 64 cases of IgG4-related disorders. *Ann Rheum Dis* 2009;**68**:1310–15.
3. **Tanaka A,** Moriyama M, Nakashima H, *et al*. Th2 and regulatory immune reactions contribute to IgG4 production and the initiation of Mikulicz disease. *Arthritis Rheum* 2012;**64**:254–63.
4. **Punnonen J,** Aversa G, Cocks BG, *et al*. Interleukin 13 induces interleukin 4-independent IgG4 and IgE synthesis and CD23 expression by human B cells. *Proc Natl Acad Sci USA* 1993;**90**:3730–4.
5. **Umehara H,** Okazaki K, Masaki Y, *et al*. Comprehensive diagnostic criteria for IgG4-related disease (IgG4-RD), 2011. *Mod Rheumatol* 2012;**22**:21–30.
6. **Iwata S,** Yamaoka K, Niiro H, *et al*. Amplification of Toll-like receptor-mediated signaling through spleen tyrosine kinase in human B-cell activation. *J Allergy Clin Immunol* 2012;**129**: 1594–601.
7. **Khosroshahi A,** Bloch DB, Deshpande V, *et al*. Rituximab therapy leads to rapid decline of serum IgG4 levels and prompt clinical improvement in IgG4-related systemic disease. *Arthritis Rheum* 2010;**62**:1755–62.
8. **Deng GM,** Liu L, Bahjat FR, *et al*. Suppression of skin and kidney disease by inhibition of spleen tyrosine kinase in lupus-prone mice. *Arthritis Rheum* 2010;**62**:2086–92.
9. **Weinblatt ME,** Kavanaugh A, Genovese MC, *et al*. An oral spleen tyrosine kinase (Syk) inhibitor for rheumatoid arthritis. *N Engl J Med* 2010;**363**:1303–12.
10. **Podolanczuk A,** Lazarus AH, Crow AR, *et al*. Of mice and men: an open-label pilot study for treatment of immune thrombocytopenic purpura by an inhibitor of Syk. *Blood* 2009;**113**:3154–60.

Amplification of Toll-like receptor–mediated signaling through spleen tyrosine kinase in human B-cell activation

Shigeru Iwata, MD, PhD,[a] Kunihiro Yamaoka, MD, PhD,[a] Hiroaki Niiro, MD, PhD,[b] Kazuhisa Nakano, MD, PhD,[a] Sheau-Pey Wang, MS,[a] Koichi Akashi, MD, PhD,[b] and Yoshiya Tanaka, MD, PhD[a] *Kitakyushu and Fukuoka, Japan*

Background: B cells are activated by combined signals through the B-cell receptor (BCR) and CD40. However, the underlying mechanisms by which BCR signals synergize with Toll-like receptor (TLR) signaling in human B cells remain unclear.
Objective: We sought to elucidate a role of spleen tyrosine kinase (Syk), a key molecule of BCR signaling, in TLR-mediated activation of human B cells.
Methods: Human naive and memory B cells were stimulated with combinations of anti-BCR, soluble CD40 ligand, and CpG. Effects of the Syk inhibitors on several B-cell functions and expression of TLR9, TNF receptor–associated factors (TRAFs), and phospho–nuclear factor κB in B cells were assessed.
Results: Activation of BCR synergized with CD40- and TLR9-mediated signals in driving robust proliferation, cell-cycle progression, expression of costimulatory molecules, cytokine production, and immunoglobulin production of human B-cell subsets, especially memory B cells. However, the Syk inhibitors remarkably abrogated these B-cell functions. Notably, after stimulation through all 3 receptors, B-cell subsets induced marked expression of *TLR9*, TRAF6, and phospho–nuclear factor κB, which was again significantly abrogated by the Syk inhibitors.
Conclusion: Syk-mediated BCR signaling is a prerequisite for optimal induction of TLR9 and TRAF6, allowing efficient propagation of TLR9-mediated signaling in memory B cells. These results also underscore the role of Syk in aberrant B-cell activation in patients with autoimmune diseases. (J Allergy Clin Immunol 2012;129:1594-601.)

Key words: *Syk, Toll-like receptor 9, TNF receptor–associated factor 6, B cells*

Abbreviations used
AICDA: Activation-induced cytidine deaminase
BCR: B-cell receptor
FITC: Fluorescein isothiocyanate
NF-κB: Nuclear factor κB
PI: Propidium iodide
SLE: Systemic lupus erythematosus
Syk: Spleen tyrosine kinase
TLR: Toll-like receptor
TRAF: TNF receptor–associated factor
XBP-1: X-box binding protein 1

B cells play a pivotal role in initiation and perpetuation of autoimmune diseases, including systemic lupus erythematosus (SLE). Activated self-reactive B cells not only are a source of pathogenic autoantibodies but also exert effector functions, including antigen presentation, cytokine production, and modulation of the T-cell repertoire. We recently reported that B-cell depletion therapy with rituximab for refractory patients with SLE not only rapidly depleted both naive and memory B cells in peripheral blood but also rapidly downregulated the expression levels of CD69, CD40 ligand, and inducible costimulator on $CD4^+$ T cells.[1] Thus B cells can facilitate autoimmune processes in both antibody-dependent and antibody-independent manners.

B cells are effectively activated by combined signals through B-cell receptor (BCR) and CD40; however, they require additional signals for efficient proliferation and differentiation. Accordingly, when combined with BCR and CD40 stimulation, Toll-like receptor (TLR) signaling by nucleic acids[2] induces the most robust B-cell activation.[3] In patients with SLE, RNA- or DNA-containing self-antigens coligate BCRs and TLR7 or TLR9, causing activation, proliferation, and differentiation of self-reactive B cells. However, the underlying mechanisms by which BCR signals potentiate TLR signaling in human B cells remain unclear.

On BCR ligation by antigens, protein kinases, including Lyn, an Src family kinase Lyn, and spleen tyrosine kinase (Syk), are initially activated.[4] Activation of Syk is a key event for further propagation of downstream signaling molecules in B cells.[5] In addition to BCR, Syk is activated through T-cell receptor and Fc receptor.[6,7] Notably, Syk inhibitors exert potent therapeutic efficacy against rheumatoid arthritis, as well as bronchial asthma and idiopathic thrombocytopenic purpura.[8-10] Moreover, Syk blockade prevents the development of skin and kidney lesions in mice with lupus.[11,12] Our current understanding of BCR-mediated Syk activation, however, extrapolates mainly from rodent studies.

In this study we demonstrate that Syk-mediated BCR signaling is a prerequisite for optimal induction of TLR9, TNF receptor–associated factor (TRAF) 6, and nuclear factor κB (NF-κB),

From [a]the First Department of Internal Medicine, University of Occupational and Environmental Health, Kitakyushu, and [b]the Department of Medicine and Biosystemic Science, Graduate School of Medical Sciences, Kyushu University, Fukuoka.

Supported in part by a Research Grant-in-Aid for Scientific Research from the Ministry of Health, Labor and Welfare of Japan; the Ministry of Education, Culture, Sports, Science and Technology of Japan; and the University of Occupational and Environmental Health, Japan.

Disclosure of potential conflict of interest: The authors declare that they have no relevant conflicts of interest.

Received for publication September 25, 2011; revised February 3, 2012; accepted for publication March 7, 2012.

Available online April 25, 2012.

Corresponding author: Yoshiya Tanaka, MD, PhD, First Department of Internal Medicine, School of Medicine, University of Occupational & Environmental Health, Japan, 1-1 Iseigaoka, Yahata-nishi, Kitakyushu 807-8555, Japan. E-mail: tanaka@med.uoeh-u.ac.jp.

0091-6749/$36.00

© 2012 American Academy of Allergy, Asthma & Immunology

doi:10.1016/j.jaci.2012.03.014

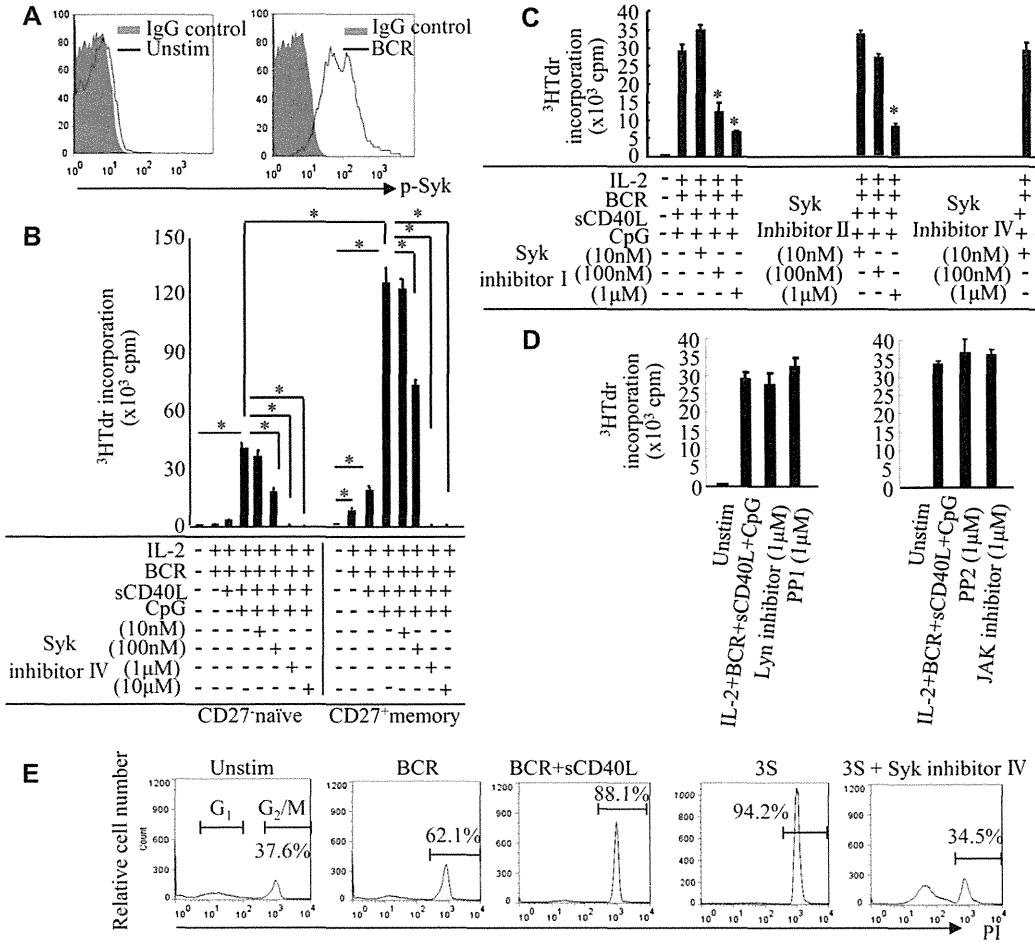

FIG 1. Syk regulates proliferation and cell-cycle progression in B-cell subsets on BCR, CD40, and TLR9 stimulation. **A**, BCR-induced phosphorylation of Syk (15 minutes). **B-D**, Tritiated thymidine *(^{3}HTdr)* incorporation of human B cells was measured during the last 18 hours of the 72-hour culture. The data are shown as means ± SDs. *$P < .05$. *sCD40L*, Soluble CD40 ligand. **E**, FACS histograms of nuclear DNA content in memory B cells 24 hours later. *Unstim*, Before stimulation; *3S*, BCR, CD40, and TLR9 stimulation. Results are representative of 3 independent experiments.

thereby driving efficient TLR9 signaling that is critical for the proliferation and differentiation of human memory B cells.

METHODS

Reagents

Syk inhibitor I, Syk inhibitor II, Syk inhibitor IV, BAY61-3606, PP1, and PP2 were purchased from Merck (Darmstadt, Germany). Lyn peptide inhibitor was purchased from Tocris Bioscience (Ellisville, Mo). PF-956980 (JAK3 kinase inhibitor) was provided from Pfizer, Inc (New York, NY). Anti-BCR mAbs (anti-Igλ and anti-Igk), recombinant human IL-2, recombinant human CD40 ligand, and phosphorothioate-protected CpG-oligonucleotide 2006 (CpG-ODN 2006; 5′-TCGTCGTTTTGTCGTTTTGTCG TT-3′) were from BD PharMingen (San Diego, Calif), R&D Systems (Minneapolis, Minn), PeproTec (Rocky Hill, NJ), and Greiner Bio-One (Tokyo, Japan), respectively.

Isolation, culture, and stimulation of B-cell subsets

This study protocol has been approved by the ethics committee of our university. PBMCs from 3 healthy donors were isolated with lymphocyte separation medium (ICN/Cappel Pharmaceuticals, Aurora, Ohio). B cells were obtained by means of negative selection from PBMCs by using the memory B-cell isolation kit (Miltenyi Biotec, Bergisch Gladbach, Germany). $CD27^+$ memory B cells were then isolated by means of positive selection from B cells with CD27 microbeads. The negative fraction of this isolation was assigned to $CD27^-$ naive B cells. Purity of naive and memory B cells was greater than 90% (see Fig E1 in this article's Online Repository at www.jacionline.org). B cells were cultured in RPMI 1640 (Wako Pure Clinical Industries, Osaka, Japan) supplemented with 10% FCS (Tissue Culture Biologicals, Tulare, Calif), 100 U/mL penicillin, and 100 U/mL streptomycin (Invitrogen, Carlsbad, Calif). According to a previous study,[13] we used the combination of anti-Igκ and anti-Igλ mAbs for BCR stimulation and initially ensured strong induction of Syk phosphorylation by these antibodies (Fig 1, *A*). CD40 stimulation with recombinant human CD40 ligand is hereafter referred to simply as CD40 stimulation. CpG-ODN 2006 is a type B CpG-ODN specific for human TLR9 and mainly activates B cells but only weakly stimulates IFN-α secretion in plasmacytoid dendritic cells.[14]

Proliferation assay

Purified B cells were stimulated in 96-well plates (1×10^5 per well) with anti-BCR mAbs (anti-Igλ and anti-Igκ, 1 μg/mL each), soluble CD40 ligand (2 μg/mL), and CpG-ODN (2.5 μg/mL) with or without IL-2 (10 ng/mL). Cells were cultured for 72 hours and pulsed with 0.5 μCi (18.5 kBq) per well of tritiated thymidine during the last 18 hours of culture and then harvested with a semiautomatic cell harvester (Abe Kagaku, Chiba, Japan), and

their uptake of tritiated thymidine was determined with a scintillation counter (Aloka LSC-3500ETM, Tokyo, Japan).

Flow cytometric analysis

After washing, B-cell subsets were incubated in blocking buffer (0.25% human globulin, 0.5% human albumin [Yoshitomi, Osaka, Japan], and 0.1% NaN_3 in PBS) in a 96-well plate at 4°C for 15 minutes. Cells were then suspended in 100 μL of FACS solution (0.5% human albumin and 0.1% NaN_3 in PBS) and treated with fluorescein isothiocyanate (FITC)–labeled murine IgG1κ, anti-human CD80 (BD PharMingen, San Diego, Calif), or anti-human CD86 (Dako Japan, Kyoto, Japan) for 30 minutes at 4°C. Cells were washed 3 times with FACS solution and analyzed with a FACSCalibur (Becton–Dickinson, San Jose, Calif) and FlowJo software (Tomy Digital Biology, Tokyo, Japan). For intracellular staining of phosho-Syk, Blimp-1, TRAF2, TRAF3, TRAF5, TRAF6, and phospho–NF-κB, cells were fixed with PBS containing 1% formaldehyde and permeabilized with saponin-PBS (PBS containing 0.1% saponin, 0.1% BSA, 0.1% NaN3, and 0.01 mol/L HEPES). After washing, cells were resuspended in saponin-PBS and stained with mouse anti-human phospho-Syk (pY348) (BD PharMingen), goat anti-human Blimp-1 (N-20; Santa Cruz Biotechnology, Santa Cruz, Calif), rat anti-human TRAF2 (MBL), rabbit anti-human TRAF3 (Santa Cruz Biotechnology), rabbit anti-human TRAF5 (Santa Cruz Biotechnology), mouse anti-human TRAF6 (Santa Cruz Biotechnology), or rabbit anti-human phospho–NF-κB p65 (Ser 536, 93H1; Cell Signaling Technology, Tokyo, Japan), followed by washing with saponin-PBS. FITC-labeled donkey anti-goat IgG (Santa Cruz Biotechnology), phycoerythrin-labeled goat anti-rat (BD PharMingen), phycoerythrin-labeled goat anti-rabbit (CALTAG), FITC-labeled rat anti-mouse (BD PharMingen), and FITC-labeled goat anti-rabbit IgG (BD PharMingen) were used as secondary antibodies. Isotype-matched goat IgG, rat IgG, rabbit IgG, or mouse IgG controls (all from Sigma-Aldrich, St Louis, Mo) were used to evaluate the background.

Apoptosis assay

Purified B cells were stimulated for 72 hours in 96-well plates (2×10^5 per well) with anti-BCR mAbs (anti-Igλ and anti-Igκ, 1 μg/mL each), soluble CD40 ligand (2 μg/mL), and CpG-ODN (2.5 μg/mL) with or without Syk inhibitor IV. After culture, cells were double-stained with FITC–Annexin V and propidium iodide (PI) in Apoptosis Detection kit I (BD PharMingen). The percentage of apoptotic cells was measured by using flow cytometry.

Cell-cycle analysis

For cell-cycle analysis, cells were suspended in PI staining buffer (50 μg/mL PI, 5 mmol/L EDTA, 1 μg/mL DNase-free RNase, and 0.1% saponin in PBS). The samples were then incubated for 30 minutes at 37°C, and DNA content was analyzed by using flow cytometry.

Cytokine production

Levels of IL-6, IL-10, IL-12 p70, and TNF-α in culture were determined by using the BD Cytometric Bead Array human Flex set, according to the manufacturer's instructions (BD PharMingen).

IgG ELISA

For quantification of *in vitro* IgG secretion, B-cell subsets were cultured with anti-BCR mAbs, CD40 ligand, and CpG-ODN 2006 in 96-well plates (1×10^5 per well) for 5 days. IgG levels in culture were determined by using a human IgG ELISA Quantitation Kit (Bethyl Laboratories, Inc, Montgomery, Ala).

Quantitative real-time PCR

Total RNA was prepared by using the RNeasy Mini Kit (Qiagen, Chatsworth, Calif). First-strand cDNA was synthesized, and quantitative real-time PCR was performed in the Step One Plus instrument (Applied Biosystems, Foster City, Calif) in triplicate wells in 96-well plates. TaqMan target mixes for X-box binding protein 1 *(XBP-1)* (Hs00152973-m1), AICDA (Hs00757808-m1), and *TLR9* (Hs00964360-m1) were purchased from Applied Biosystems. *XBP-1*, activation-induced cytidine deaminase *(AICDA)* and *TLR9* mRNA expression levels were normalized to the levels of 18S ribosomal RNA (Hs99999901-m1, Applied Biosystems) as an endogenous control, and the relative quantity compared with the PBMC sample as a reference was calculated by using the quantification-comparative cycle threshold ($\Delta\Delta C_T$) formula. Relative quantity was calculated by using the $\Delta\Delta C_T$ formula–referenced sample of PBMCs.

Western blot analysis

Raji cells were lysed in an NP-40 buffer containing NaCl, Tris-HCL (pH 8.0), distilled water, and protease inhibitor. Lysates were then mixed with an equal volume of sample buffer solution (2-mercaptoethanol; Wako Pure Chemical Industries) and boiled for 5 minutes. Proteins were separated by means of SDS-PAGE, transferred onto nitrocellulose membranes (Whatman, Tokyo, Japan), blocked with 5% skim milk, and immunoblotted with anti-human Syk, anti-human phospho-Syk (pY348), anti-human TRAF6, anti-human phospho–NF-κB p65 (Ser 536, 93H1), and horseradish peroxidase–labeled anti-secondary (#NA931V and #NA934V; GE Healthcare, Osaka, Japan) by using immunoreaction enhancer solution (Can Get Signal; Toyobo, Osaka, Japan). Blots were developed with ECL Western Blotting Detection Reagents (GE Healthcare) and visualized with a light-capture instrument (ATTO, Tokyo, Japan).

Statistical analysis

All statistical analyses were performed with JMP version 8.0.2 statistical software (SAS Institute Inc, Cary, NC). Statistical significance of differences between the pretreatment and posttreatment values was tested by using the Wilcoxon test. *P* values of less than .05 were considered statistically significant.

RESULTS

Syk is critical for proliferation and cell-cycle progression in memory B cells

We investigated the effect of BCR, CD40, and TLR9 stimulation on the proliferation of B-cell subsets. BCR stimulation alone remarkably induced Syk phosphorylation; however, it had only marginal effects on DNA synthesis in B cells (Fig 1, *A* and *B*). Combined stimulation of BCR, CD40, and TLR9 strongly induced DNA synthesis in both naive and memory B cells, although significantly more so in the latter. This robust proliferation was inhibited by Syk inhibitor IV (BAY61-3606) in a dose-dependent manner (Fig 1, *B*). Similar data were obtained with another Syk inhibitor (Syk inhibitors I and II; Fig 1, *C*). In contrast to these Syk inhibitors, non-Syk inhibitors (PP1, PP2, and JAK inhibitor) were not effective, even at high concentrations (Fig 1, *D*). Syk inhibitor IV was hereinafter used for further experiments. We next tested cell-cycle progression in memory B cells after BCR, CD40, and TLR9 stimulation (Fig 1, *E*). The percentage of cells in the G_2/M phase without stimulation was 37.6%. This value increased further up to 94.2% with combined stimulation of BCR, CD40, and TLR9. Consistent with our results (Fig 1, *B* and *C*), Syk inhibitor IV significantly inhibited G_2/M phase progression in memory B cells. Together, these results suggest a critical role for Syk in BCR-, CD40-, and TLR-induced proliferation and cell-cycle progression in human memory B cells.

Syk regulates expression of costimulatory molecules and cytokine production in B-cell subsets

We tested expression of the costimulatory molecules CD80 and CD86 in B cells (Fig 2). Both were only marginally expressed in

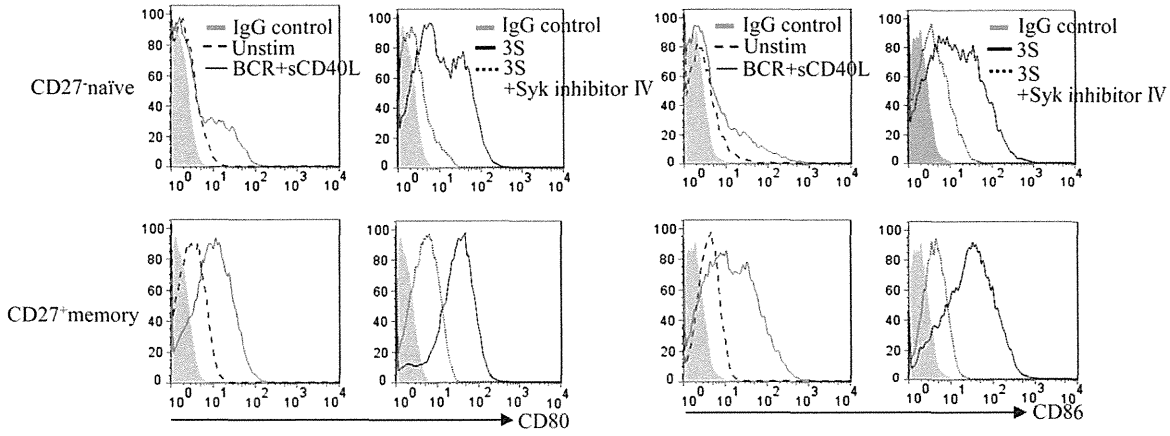

FIG 2. Syk regulates expression of CD80 and CD86 in B-cell subsets on stimulation. *Overlay histograms* depict relative fluorescence intensities of human naive and memory B cells cultured for 72 hours. *Unstim*, Before stimulation; *3S*, BCR, CD40, and TLR9 stimulation. Results are representative of 3 independent experiments.

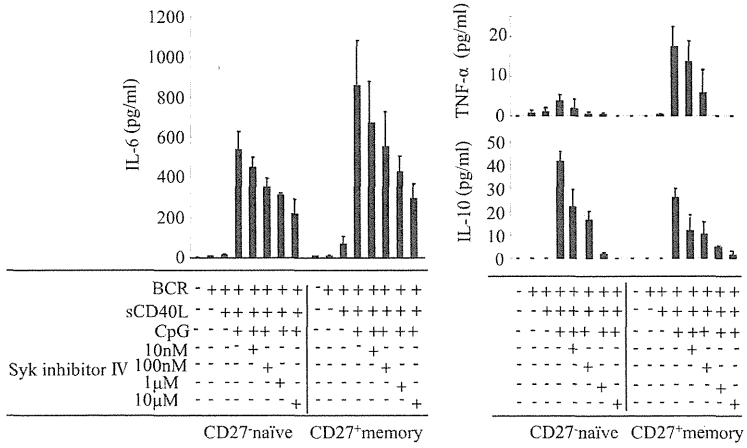

FIG 3. Syk regulates cytokine production in B-cell subsets on stimulation. Human peripheral blood naive and memory B cells were cultured for 72 hours, and supernatants were harvested and assayed by using the cytometric bead array for IL-6, TNF-α, and IL-10 content. Data are shown as means ± SDs and are representative of 3 independent experiments. *sCD40L*, Soluble CD40 ligand.

memory but not naive B cells without stimulation. Combined stimulation of BCR, CD40, and TLR9 induced significant expression of CD80/CD86 in memory B cells compared with that seen in naive cells. Syk inhibitor IV almost completely canceled CD80/CD86 expression in both subsets, suggesting a role of Syk in expression of costimulatory molecules in B cells.

We next analyzed cytokine production (IL-6, IL-10, and TNF-α) by B-cell subsets (Fig 3). Combined stimulation with BCR, CD40, and TLR9 induced production of the proinflammatory cytokines IL-6 and TNF-α in naive and memory cells, although more markedly in the latter. Syk inhibitor IV clearly inhibited production of these cytokines in both subsets in a dose-dependent fashion. In contrast to proinflammatory cytokines, anti-inflammatory IL-10 production was more pronounced in naive than memory B cells, which is consistent with a recent study that IL-10–producing B cells are enriched in human $CD27^{-}CD38^{hi}$ B cells.[15] Again, dose-dependent suppression of IL-10 production by Syk inhibitor IV was observed in both subsets. We failed to detect IL-12 p70, IL-2, IFN-α, and IFN-γ under any conditions (data not shown). These results suggest the critical role of Syk in BCR-, CD40-, and TLR-induced cytokine production in B-cell subsets and also underscore the therapeutic efficacy of Syk inhibitors in decreasing the inflammatory consequences of autoimmune diseases by modulating proinflammatory cytokines, such as TNF-α and IL-6.

Syk regulates B-cell differentiation on BCR, CD40, and TLR9 stimulation

On strong stimulation, B cells differentiate to plasma cells and undergo class-switching along with expression of critical molecules, such as *AICDA*, *XBP-1*, and Blimp-1. Both naive and memory B cells strongly induced expression of *AICDA*, *XBP-1*, and Blimp-1 after BCR, CD40, and TLR9 stimulation, which was inhibited by Syk inhibitor IV (Fig 4, *A* and *B*). In addition, IgG production induced by BCR, CD40, and TLR9 stimulation, which was particularly high in memory B cells, was again greatly reduced by Syk inhibitor IV in a dose-dependent manner (Fig 4, *C*).

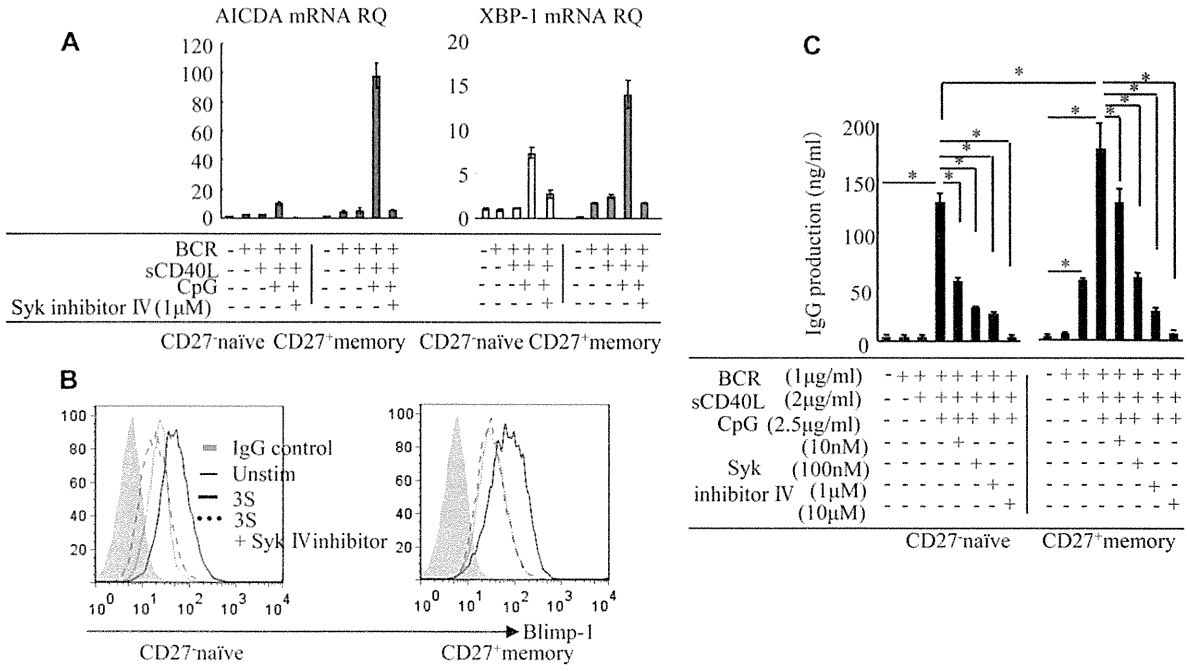

FIG 4. Syk regulates B-cell differentiation on BCR, CD40, and TLR9 stimulation. Naive and memory B cells were cultured for 48 hours (*AICDA* and *XBP-1* mRNA and Blimp-1) or for 5 days (IgG production). **A**, The level of *AICDA* and *XBP-1* mRNA was measured by using real-time PCR. *RQ*, Relative quantity. **B**, Blimp-1 expression was measured by means of flow cytometry. *Unstim*, Before stimulation; *3S*, BCR, CD40, and TLR stimulation. **C**, IgG in the supernatant was quantified by using ELISA. Data are shown as means ± SDs and are representative of 3 independent experiments. $*P < .05$. *sCD40L*, Soluble CD40 ligand.

These results suggest that Syk also regulates B-cell differentiation induced by BCR, CD40, and TLR9 stimulation.

TRAF6 is a key Syk-regulated molecule in B-cell subsets on stimulation

Syk is a key downstream signaling molecule of BCR, but not CD40 or TLR9, in B cells.[16,17] Considering that Syk blockade significantly abrogates proliferation, cytokine production, and differentiation after BCR, CD40, and TLR9 stimulation (Figs 1-4), we particularly sought to elucidate the mechanisms by which Syk regulates TLR9 signaling in human B-cell subsets. Given that TLR9 expression is significantly induced in BCR-stimulated B cells and that TRAFs are the critical downstream molecules in CD40 and TLR9 signaling in B cells,[18,19] we reasoned that TLR9 and TRAFs were possible candidates. Memory B cells constitutively expressed more *TLR9* mRNA than naive B cells (Fig 5, *A*). On BCR, CD40, and TLR9 stimulation, *TLR9* mRNA expression was more drastically induced in memory than naive B cells. Syk inhibitor IV inhibited expression of *TLR9* mRNA in memory B cells to the level seen in unstimulated naive B cells (Fig 5, *A*). Among TRAFs, expression of TRAF2, TRAF3, and TRAF5 was constitutively detected; however, their expression was not affected by BCR stimulation (Fig 5, *B*). In contrast, TRAF6 expression was only slightly detected in memory B cells without stimulation. BCR stimulation alone, however, potently increased TRAF6 expression in both subsets (Fig 5, *B*). TRAF6 expression was further pronounced by additional CD40 and TLR9 stimulation, and strong NF-κB phosphorylation was correlatively observed. Expression of these molecules was blocked by Syk inhibitor IV (Fig 5, *B* and *C*).

Without stimuli, Raji cells exhibit higher basal (tonic) signaling that supports proliferation and survival.[20] In these cells TLR9 mRNA was expressed at a much higher level than in unstimulated naive B cells, which was markedly reduced by Syk inhibitor IV (Fig 6, *A*). In addition, these cells constitutively exhibited pronounced expression and phosphorylation of Syk. Syk inhibitor IV clearly inhibited Syk phosphorylation without affecting its protein levels. Of note, TRAF6 expression and NF-κB phosphorylation were strongly reduced as well by Syk inhibitor IV (Fig 6, *B*). These suggest that Syk blockade exerts an inhibitory action on expression of TLR9, TRAF6, and NF-κB phosphorylation, even in B cells with high basal BCR signaling.

DISCUSSION

In this study we demonstrate that engagement of BCR in conjunction with ligation of CD40 and TLR9 induces remarkable proliferation, expression of costimulatory molecules, cytokine production, and immunoglobulin production in human B cells, especially the memory subset. Moreover, the Syk inhibitor suppresses all of these functions to background levels, at least in part through inhibition of expression of TLR9 and TRAF6, resulting in decreased phosphorylation of NF-κB.

We show that combined stimulation with BCR and CD40 was sufficient to activate memory B cells, whereas it had less effect on naive B cells. However, Additional CpG stimulation caused potent activation of both subsets, although always more strongly in the memory subset, suggesting that memory B cells exhibit a lower threshold for activation compared with naive B cells. Memory B cells can survive without antigenic stimulation, and they can be fully activated only by cognate T-cell help and

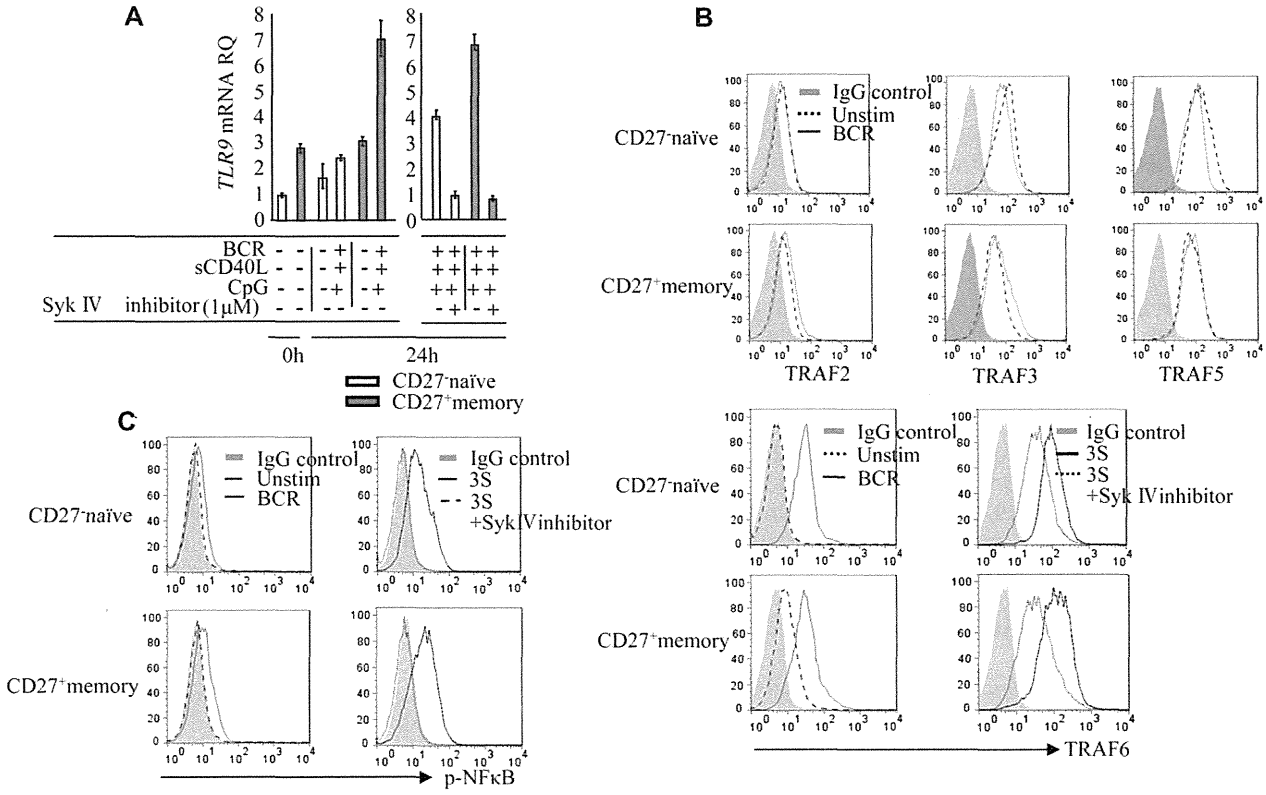

FIG 5. TLR9 and TRAF6 are key Syk-regulated molecules in B-cell subsets on stimulation. **A**, *TLR9* mRNA was quantified by using real-time PCR (TaqMan PCR kit) 24 hours later. *RQ*, Relative quantity; *sCD40L*, soluble CD40 ligand. **B** and **C**, TRAF2, TRAF3, TRAF5, and TRAF6 levels (48 hours later) and NF-κB phosphorylation (p65; 12 hours later) were measured by means of flow cytometry (intracellular staining). *Unstim*, Before stimulation; *3S*, combination of BCR, CD40, and TLR9 stimulation. Data are representative of 3 independent experiments.

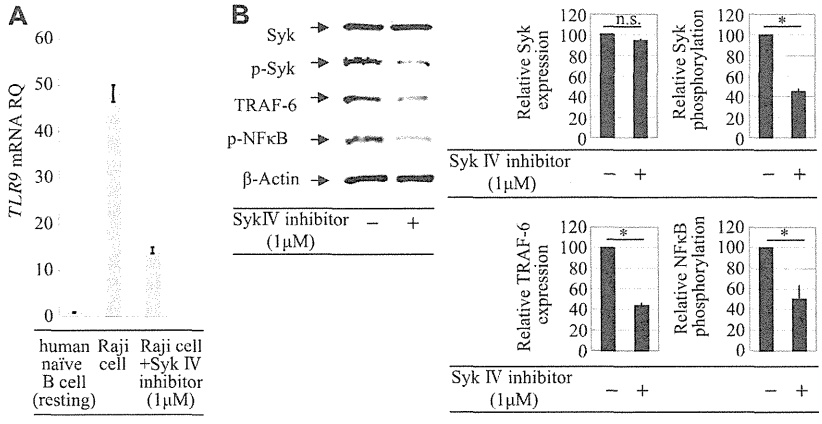

FIG 6. Syk inhibitor exerts marked inhibitory action, even at an activated state of B cells. Raji cells were cultured with RPMI containing 2% FCS for 48 hours. **A**, *TLR9* mRNA was quantified by means of real-time PCR. *RQ*, Relative quantity. **B**, Expression of Syk, phospho-Syk (Y348), TRAF6, and phospho-NF-κB (p65) was assessed by means of Western blotting. The intensity of bands was quantified and normalized with respect to those of corresponding β-actin. The resulting values were expressed as the percentage in reference to that of cells without Syk inhibitor IV. Data are shown as means ± SDs and are representative of 3 independent experiments. $*P < .05$. *n.s.*, Not significant.

cytokines.[21-23] In addition, the costimulatory molecules CD80 and CD86, as well as TLR9 and TRAF6, are weakly expressed in memory B cells in the nonstimulated (steady) state (Figs 2 and 5). These findings suggest that a basal BCR tonic signal in memory B cells is higher than in naive B cells, which might account for the maintenance of serologic memory.[24,25]

What signaling molecules are responsible for a basal BCR tonic signal in memory B cells? We recently showed that without

BCR stimulation, weak activation of Syk is constitutively observed in memory B cells.[26] Given that Syk activation is a key event for further propagation of the BCR signaling pathway,[4] these findings support our rationale that blockade of Syk activation regulates the functions of memory B cells. Surprisingly, the effects of the Syk inhibitor on B-cell functions were more dramatic than we had initially expected: it almost completely abrogated B-cell proliferation, activation, cytokine production, and differentiation induced by a combinatorial stimulation of BCR, CD40, and TLR9 (Figs 1-4). We also evaluated B-cell survival by determining the percentage of apoptotic cells with FITC–Annexin V and PI. Consistent with our previous study,[26] without stimuli, a considerable fraction of B cells spontaneously underwent apoptotic cell death *in vitro*, and such cell death was not affected by the Syk inhibitor, excluding nonspecific cytotoxic effects of this inhibitor on B-cell survival (see Fig E2 in this article's Online Repository at www.jacionline.org). On stimulation with BCR, CD40, and TLR9, apoptotic cell death (Annexin V^+PI^- and AnnexinV^+PI^+) was considerably protected. This protection was indeed abrogated by the Syk inhibitor in a dose-dependent manner, suggesting that Syk provides survival signals as well for B cells after stimulation through all 3 receptors (see Fig E2).

It remains somewhat unclear whether Syk is directly activated in CD40 and TLR9 signaling pathways in B cells.[16,17] Ying et al[27] showed that Syk is synergistically activated in B cells on BCR/CD40 costimulation, suggesting a role for Syk in CD40 signaling. Sanjuan et al[28] showed, using human monocytic cell lines, that tyrosine phosphorylation of TLR9 by the Src family kinases leads to the recruitment and activation of Syk, suggesting a role for Syk in TLR9 signaling. In contrast to these findings, we found that robust proliferation in memory B cells after CD40, TLR9, or both stimulation is not influenced by the Syk inhibitor (data not shown). Thus other regulatory mechanisms of B-cell activation by the Syk inhibitor are more likely to exist.

We show here that Syk is a regulator of expression of TLR9 and TRAF6, both of which are critical for TLR9-induced NF-κB activation. Consistent with our results, a previous study showed that *TLR9* mRNA is expressed at high levels in memory B cells and its expression is enhanced by BCR cross-linking,[18] although involvement of Syk in this process was not investigated. NF-κB activation regulates *TLR9* mRNA expression induced by BCR, CD40, and TLR9 stimulation,[29] suggesting that NF-κB–induced TLR9 expression forms a novel feed-forward loop in NF-κB activation in B cells. Blockade of Syk-mediated BCR signaling could thus shut off this loop, thereby inhibiting NF-κB activation and TLR9 expression. Indeed, we found that Syk inhibition reduces expression of TLR9 mRNA in memory B cells to the levels seen in unstimulated, steady-state naive B cells (Fig 5, *A*).

TRAF6 plays a pivotal role in TLR9-induced c-Jun N-terminal kinase activation, CD80 expression,[30] and IL-6 production.[31] B cell–specific disruption of TRAF6 results in a lower number of mature B cells, as well as inhibition of antibody class-switching and impaired differentiation to plasma cells.[32] We found that BCR stimulation alone strongly induces TRAF6 expression, which is further enhanced by additional CD40 and TLR9 stimulation (Fig 5, *B*). TRAF6 expression, as well as NF-κB phosphorylation, on B-cell activation is markedly inhibited by Syk blockade. These findings clearly suggest that Syk-mediated BCR signaling is a prerequisite for optimal induction of TRAF6, allowing efficient propagation of TLR9 signaling.

Our current findings provide a novel insight into B-cell aberrations in patients with SLE. The prevailing hypothesis of B cell–mediated autoimmunity is that both autoantigen-triggered BCR signals and costimulatory signals are required for activation of autoreactive (pathogenic) B cells, which are particularly enriched in the memory subset. However, recent studies showed that TLR7 and TLR9 can recognize self-derived RNA and DNA, respectively, and that TLR signaling is necessary for autoantibody production in mice with lupus.[33,34] BCR-induced calcium mobilization and protein tyrosine phosphorylation were both pronounced in B cells from mice with SLE,[35] indicating that alterations in B-cell signaling already occur at the proximity of the BCR. We here demonstrate that Syk-mediated BCR signaling is a prerequisite for optimal induction of TLR9 and TRAF6, thereby allowing efficient propagation of CD40 and TLR9 signaling, which are critical for the proliferation and differentiation of human memory B cells. Our current findings also underscore the potential role of Syk in B cell–mediated pathologic processes in patients with autoimmune diseases, namely Syk-mediated BCR signaling, could be already activated probably by autoantigens and that Syk inhibitors have potential as new drugs in the treatment of autoimmune diseases, including SLE and RA.

We thank Ms T. Adachi, Ms N. Sakaguchi, and Ms K. Noda for their excellent technical assistance.

Clinical implications: Syk inhibitors might be promising for controlling the aberrant TLR9 signaling that is related to the proliferation and differentiation of pathogenic memory B cells in patients with autoimmune diseases, including SLE and RA.

REFERENCES

1. Iwata S, Saito K, Tokunaga M, Yamaoka K, Nawata M, Yukawa S, et al. Phenotypic changes of lymphocytes in patients with systemic lupus erythematosus who are in longterm remission after B cell depletion therapy with rituximab. J Rheumatol 2011;38:633-41.
2. Krug A. Nucleic acid recognition receptors in autoimmunity. Handb Exp Pharmacol 2008;183:129-51.
3. Ruprecht CR, Lanzavecchia A. Toll-like receptor stimulation as a third signal required for activation of human naïve B cells. Eur J Immunol 2006;36:810-6.
4. Taniguchi T, Kobayashi T, Kondo J, Takahashi K, Nakamura H, Suzuki J, et al. Molecular cloning of a porcine gene syk that encodes a 72-kDa protein-tyrosine kinase showing high susceptibility to proteolysis. J Biol Chem 1991;266:15790-6.
5. Kulathu Y, Grothe G, Reth M. Autoinhibition and adapter function of Syk. Immunol Rev 2009;232:286-99.
6. Wong WS, Leong KP. Tyrosine kinase inhibitors: a new approach for asthma. Biochim Biophys Acta 2004;1697:53-69.
7. Beaven MA, Baumgartner RA. Downstream signals initiated in mast cells by Fc epsilon RI and other receptors. Curr Opin Immunol 1996;8:766-72.
8. Meltzer EO, Berkowitz RB, Grossbard EB. An intranasal Syk-kinase inhibitor (R112) improves the symptoms of seasonal allergic rhinitis in a park environment. J Allergy Clin Immunol 2005;115:791-6.
9. Podolanczuk A, Lazarus AH, Crow AR, Grossbard E, Bussel JB. Of mice and men: an open-label pilot study for treatment of immune thrombocytopenic purpura by an inhibitor of Syk. Blood 2009;113:3154-60.
10. Weinblatt ME, Kavanaugh A, Genovese MC, Musser TK, Grossbard EB, Magilvay DB. An oral spleen tyrosine kinase (Syk) inhibitor for rheumatoid arthritis. N Engl J Med 2010;363:1303-12.
11. Bahjat FR, Pine PR, Reitsma A, Cassafer G, Baluom M, Grillo S. An orally bioavailable spleen tyrosine kinase inhibitor delays disease progression and prolongs survival in murine lupus. Arthritis Rheum 2008;58:1433-44.
12. Deng GM, Liu L, Bahjat FR, Pine PR, Tsokos GC. Suppression of skin and kidney disease by inhibition of spleen tyrosine kinase in lupus-prone mice. Arthritis Rheum 2010;62:2086-92.
13. Sakurai D, Kanno Y, Hase H, Kojima H, Okumura K, Kobata T. TACI attenuates antibody production costimulated by BAFF-R and CD40. Eur J Immunol 2007;37:110-8.